UNCLASSIFIED

AD NUMBER

AD801308

NEW LIMITATION CHANGE

TO

Approved for public release, distribution unlimited

FROM

Distribution authorized to U.S. Gov't. agencies and their contractors; Administrative/Operational Use; JAN 1953. Other requests shall be referred to Defense Nuclear Energy, Washington, DC.

AUTHORITY

DNA/IMTI memo, 5 May 1974

THIS PAGE IS UNCLASSIFIED

UNCLASSIFIED

AD NUMBER
AD801308
CLASSIFICATION CHANGES
TO unclassified
FROM restricted
AUTHORITY
23 Oct 1958, per doc markings

THIS PAGE IS UNCLASSIFIED

WT-509

801308

801308

DDC FILE COPY

CONFIDENTIAL
Security Information

UNCLASSIFIED

WT-509

This document consists of 69 pages
No. 258 of 357 copies, Series A

(18) AEC
(19) WT-509

(21) Report on
Project 3.3.

(6)

BLAST DAMAGE TO TREES — ISOLATED CONIFERS.

REPORT TO THE TEST DIRECTOR

(10)
A. A. Brown, [redacted]
R. K. Arnold,
W. L. Fons,
F. M. Sauer
W. E. Reifsnyder

DDC
RECEIVED
NOV 7 1966
C

(12) 61p.

(11) Jan[redacted]53

Classification cancelled (or changed to UNCLASSIFIED)

by authority of TID-9027

by [illegible], date 10-23-58

~~Division of Fire Research~~
Forest Service, U. S. Department of Agriculture
Wash D. C.

UNCLASSIFIED

CONFIDENTIAL
Security Information

RESTRICTED DATA
ATOMIC ENERGY ACT 1946

141 750

ABSTRACT

Project 3.3, aiming at prediction of blast damage to forests from atomic explosions, sought to establish the following relationships for isolated coniferous trees: (1) Tree damage in terms of stem breakage, branch breakage, and defoliation in relation to peak overpressure and positive phase duration time; (2) deflection-time and strain-time functions for tree stems following arrival of shock wave.

Four pine trees and a weighted disk on an aluminum beam (called lollipop) were exposed at each of four stations. Trees approximately 45 ft high and 12 in. in diameter were cut from the Nevada National Forest and placed in concrete foundations at the test site. Lollipops, 32 in. in diameter and weighing 380 lb, were mounted 14 ft above the ground on 4-in. aluminum I-beams, which in turn were fixed in concrete foundations. Strain meter-oscillograph systems recorded strain-time relationships on one tree and the lollipop at each station. Motion pictures were used to scale deflection-time data. On each tree scratch gages recorded maximum strain at base of crown and at 1-ft level, and snubber wires measured maximum stem deflection at a selected reference point.

Six trees were broken on Shot 3 and one of the remaining on Shot 4. No defoliation or branch breakage occurred; tree crowns broke up as a unit with a stem break usually near the base of the crown. This tree breakage was related with two ratios: shock peak dynamic pressure to dynamic pressure for breakage due to steady wind; and tree period to positive phase duration time. Lollipop deflection-time history was also related to the latter ratio and to the ratio of maximum deflection to static deflection associated with peak dynamic pressure.

Good agreement was found between Shot 3 lollipop deflections and those theoretically predicted using measured overpressures. Breakage and deflection data on Shot 4 indicate that actual peak dynamic pressure was greater than that calculated from peak overpressure. This observation agrees with Sandia Laboratory dynamic pressure measurements and Los Alamos Scientific Laboratory smoke velocity data.

Blast damage to forests from atomic explosions is primarily a function of aerodynamic drag associated with particle velocity. Peak dynamic pressure is a more compatible parameter than peak overpressure for predicting blast damage to trees and other structures which have comparatively long periods and are susceptible to damage by aerodynamic drag. The lower limit of peak dynamic pressure for complete breakage of isolated conifers is estimated to be in the order of 0.7 psi when associated with 1-sec positive phase duration. This value of dynamic

Cont p. 4

pressure corresponds to a sea level overpressure of 5.5 psi for Mach reflection. Some breakage will occur at lower peak dynamic pressures because of strength variations in tree stems.

Natural forests or prepared forest stands can be instrumented economically to study blast damage from atomic explosions with no requirement for outside power or timing signals.

It is recommended that more static breakage tests be made to establish variations in static strength of growing tree stems, and that future effects tests consist of a graded series of shots to increase the range of duration times as well as overpressures.

RESTRICTED DATA
ATOMIC ENERGY ACT 1946

CONTENTS

ABSTRACT 3

ILLUSTRATIONS. 7

TABLES 8

CHAPTER 1 OBJECTIVE. 9

CHAPTER 2 BACKGROUND AND THEORETICAL DATA. 10

2.1 General 10
2.2 Computation System. 11

CHAPTER 3 PREPARATIONS AND METHODS 13

3.1 Stations and Trees. 13
3.2 Lollipops 19
3.3 Instrumentation 20
3.3.1 Strain-Time Measurement. 20
3.3.2 Maximum Strain Measurement 24
3.3.3 Maximum Deflection Measurement 24
3.3.4 Motion Pictures. 24

CHAPTER 4 RESULTS. 25

4.1 General 25
4.2 Deflection, Time History — Trees 27
4.3 Maximum Deflection — Lollipops 34
4.4 Scratch Gage Strain Measurement 34

CHAPTER 5 DISCUSSION 38

5.1 General 38
5.1.1 Correlation of Shot 3 Lollipop Data. . . . 38
5.1.2 Comparison of Shot 3 and Shot 4 Results. . 39
5.2 Tree Breakage 40
5.3 Deflection-Time History — Trees. 41
5.4 Deflection-Time History — Lollipops. 43
5.5 Scratch Gage Data 44
5.6 Instrumentation 45
5.6.1 Snubbers 45
5.6.2 Scratch Gages. 45
5.6.3 Oscillograph-Strain System 45
5.6.4 Motion Pictures. 45
5.6.5 Lollipops. 46

CHAPTER 6 CONCLUSIONS AND RECOMMENDATIONS. 47

6.1 Conclusions 47
6.2 Recommendations 48
6.2.1 Future Atom Bomb Field Tests 48
6.2.2 Other Work. 49

APPENDIX A CALCULATION METHODS. 50

A.1 Equation of Motion —Lollipops. 50
A.2 Peak Particle Velocity and Density From Shock Equations 54
A.2.1 Regular Reflection 54
A.2.2 Mach Reflection. 57
A.3 Reduction of Deflection Data — Lollipops 57
A.4 Equation of Motion — Trees 58
A.5 Reduction of Breakage Data — Trees 58

NOMENCLATURE 60

ILLUSTRATIONS

2.1 Calculated Breakage Overpressures for Isolated Ponderosa Pine 12

2.2 Normalized Breakage Shock Pressure Ratio for Isolated Ponderosa Pine. 12

3.1 Station I Showing Lollipop and Trees 13

3.2 Station II Showing Lollipop and Trees. 14

3.3 Station III Showing Lollipop and Trees 14

3.4 Station IV Showing Lollipop and Trees. 14

3.5 Plot Plan and Station Layout 15

3.6 Static Strain, Load, Deflection Relationships for Instrumented Trees 18

3.7 Lollipop at Station I. 19

3.8 Strain Meter 21

3.9 Strain Meter Mounted on Tree 21

3.10 Block Diagram — Oscillograph Power and Relay Systems. . . . 22

3.11 Photo Cell and Mount Above Instrument Shelter. 23

3.12 Station I Viewed From Motion Picture Camera Station. 24

4.1 Breakage of Trees B, C, D at Station II, Shot 3. 26

4.2 Typical Stem Failures. 27

4.3 Regions of Breakage and Non-Breakage—Conifers, Shot 3 . . . 28

4.4 Regions of Breakage and Non-Breakage—Conifers, Shot 4 . . . 28

4.5 Tracing of Strain Meter Record, Tree I A, Shot 3 30

4.6 Motion of Reference Point Under Blast Loading, Tree I A, Shot 2 30

4.7 Motion of Reference Point Under Blast Loading—Trees, Shot 3. 31

4.8 Motion of Reference Point Under Blast Loading—Trees, Shot 4. 32

4.9 Normalized Lollipop Maximum Deflection and Time to Maximum Deflection, Shots 2, 3, and 4. 35

4.10 Scratch Gage Record and Diagrammatic Explanation 36

4.11 Comparison of Strain Measurement—Scratch Gage Versus Strain Meter. 36

A.1 Equivalent Mechanical System—Lollipop 50

A.2 Theoretical Particle Velocity and Density Variation With Time for Free Air 53

A.3 Incident-Reflected Shock in Stationary Frame of Reference. . 54

TABLES

3.1 Mechanical Characteristics of Trees. 16

3.2 Physical Characteristics of Trees. 17

3.3 Lollipop Characteristics 20

4.1 Overpressures and Positive Phase Duration Times. 25

4.2 Characteristics and Circumstances of Tree Breakage 26

4.3 Oscillograph Time of Arrival and Film Speed Data 29

4.4 Maximum Tree Deflections 33

4.5 Maximum Lollipop Deflections 34

4.6 Maximum Strain Comparison—Scratch Gages and Strain Meters . 37

5.1 Range of Variables Covered by Deflection Calculations . . . 43

RESTRICTED DATA
ATOMIC ENERGY ACT 1946

CHAPTER 1

OBJECTIVE

Project 3.3 was one phase in a research program aimed at prediction of blast damage to forests from atomic explosions. Studies connected with Project 3.3 were confined to isolated coniferous trees in order to simplify the problem and to establish the following relationships, which provide a field check on blast damage prediction:

1. Tree damage in terms of stem breakage, branch breakage, and defoliation in relation to peak overpressure and positive phase duration time.

2. Deflection-time and strain-time functions for tree stems following arrival of shock wave.

To provide a further check on computational systems used for damage prediction, deflection- and strain-time relations were measured on a simple spring-mass system which was designed to represent an "ideal-reproducible" tree.

These studies of isolated coniferous stems were preliminary to more comprehensive projects which deal with tree stands of varying densities, shapes, and combinations of tree species. Therefore it was important for Project 3.3 to develop and field-test methods and techniques of measuring motion and strain on tree stems subject to blast from atomic explosions in order to instrument a forest stand at reasonable cost.

CHAPTER 2

BACKGROUND AND THEORETICAL DATA

2.1 GENERAL

Preliminary analysis[1] of damage to trees by shock wind indicated that at sea level, conifers 24-in. DBH[2] with 50 per cent crown and a natural period of 2.5 sec would be expected to break at an overpressure of approximately 7.5 psi in the Mach stem region. The purpose of this preliminary work was more to develop methods of analysis and delineate problem parameters than to establish a radius of tree breakage. This analysis provided the basis for several field studies which followed.

Studies of aerodynamic drag in tree crowns[3] indicated the nature of forces which blast winds from atomic explosions might exert on isolated tree crowns. Variation in tree crown drag was found to be due primarily to bending upon application of drag force. Dry weight of crown appeared to be the best parameter with which drag could be correlated.

Bending and breakage characteristics of ponderosa pine stems subjected to static loading have been analyzed,[4] and indicate that maximum stress at the point of static failure is of the order of 3,000 lb/sq in. Trees subjected to static loading near the center of pressure of the crown generally broke near the base of crown.

1/ Operations Research Office. Preliminary Study of the Consequences of an Atomic Explosion Over a Forest. ORO-T-108. Washington, 1950. 102 pp.

2/ Diameter at breast height, 4-1/2 ft above the ground, outside bark.

3/ U. S. Dept. of Agriculture, Forest Service, Division of Fire Research. Experimental Investigation of Aerodynamic Drag in Tree Crowns Exposed to Steady Wind—Conifers. Phase Report for Operations Research Office. December 20, 1951. 19 pp.

4/ U. S. Dept. of Agriculture, Forest Service, Division of Fire Research. Tree Breakage Characteristics Under Static Loading--Ponderosa Pine. Report in preparation for Armed Forces Special Weapons Project.

RESTRICTED DATA
ATOMIC ENERGY ACT 1946

2.2 COMPUTATION SYSTEM

Further analysis of tree-stem breakage by shock wind,[5] which employed data from work described above, established significant parameters of tree characteristics and shock wave characteristics which affect the probability of breakage and blow-down following atomic explosions.

In this analysis the tree was replaced by a single-mass, spring-mass system with the mass placed at the position of the center of pressure of the crown drag force. Natural period of the simplified system equaled that of the tree, and the mass had the drag associated with the crown. Restoring force characteristics of the spring were determined from static deflection measurements made on the tree stem. The viscous damping constant was determined from damped free vibration of the stem.

The equation of motion equates drag, restoring, and damping forces to the inertial force

$$m \frac{dy^2}{dt^2} = \rho \frac{V^2}{2} D(y) - R(y) - \alpha \frac{dy}{dt} \qquad (2.1)$$

where V is the relative velocity between the shock particle velocity and the velocity of the mass center, y is the displacement of the mass center, and ρ is the air density. Density and particle velocity are assumed to have a linear function with time. Equation 2.1 was then numerically integrated in the manner outlined by Timoshenko.[6] Figures 2.1 and 2.2, results of calculations made to date, were used to locate stations for Project 3.3. Similar calculations were made on weighted beams to predict maximum deflections for each shot. These calculations were used to determine strength requirements and strain recorder gain settings. A more detailed presentation of the method is in Appendix A.

5/ U. S. Dept. of Agriculture, Forest Service, Division of Fire Research. Analysis of Tree-Stem Breakage by Shock Wind--Ponderosa Pine. Report in preparation for Armed Forces Special Weapons Project.
6/ Timoshenko, S. Vibration Problems in Engineering. (2nd ed.), New York: D. VanNostrand Co., Inc., 1937. p. 126.

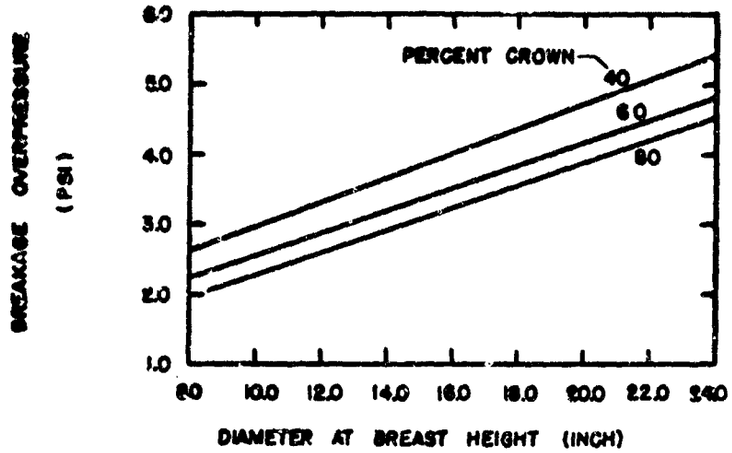

Fig. 2.1 Calculated Breakage Overpressures for Isolated Ponderosa Pine. Based on Sea Level Free Air Overpressures for a 20 KT Bomb at 2,000 Ft Burst Height.

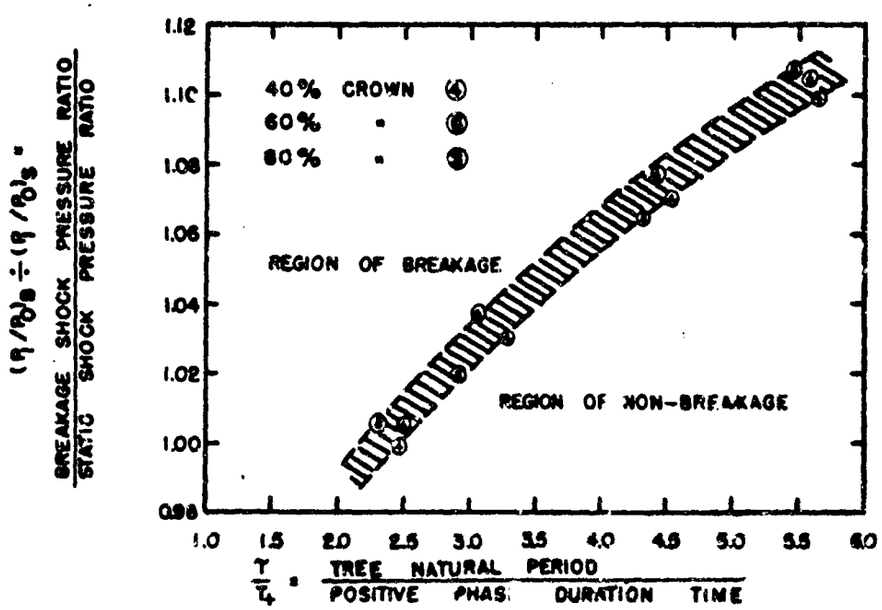

Fig. 2.2 Normalized Breakage Shock Pressure Ratio for Isolated Ponderosa Pine. Static Shock Pressure Ratio Based on Shock Peak Dynamic Pressure Equal to That Associated With Breakage Due to Steady Wind as Calculated From Normal Shock Relationships.

RESTRICTED DATA
ATOMIC ENERGY ACT 1946

CHAPTER 3

PREPARATIONS AND METHODS

3.1 STATIONS AND TREES

Four trees and a "lollipop"[1/] were placed at each of four stations on the Forest Service line in Area 7. Stations covered a range of 1.9 to 5.3 psi peak overpressure for Shots 3 and 4 as shown in Table 4.1. Figures 3.1, 3.2, 3.3, and 3.4 are station photographs. The plot plan and station layout are shown in Fig. 3.5.

Fig. 3.1 Station I Showing Lollipop and Trees A, B, C, and D (Left to Right) With Crowns 40, 60, 80, and 30 Per Cent of Total Height. View From Direction of Ground Zero.

Trees, approximately 45 ft high and 12 in. DBH, were cut from Site Class 4 and 5 areas on the Charleston Ranger District of the Nevada National Forest. Whole trees were hauled by special trailer to the Nevada Proving Grounds and anchored by placing butt-ends 6 ft into prepared concrete foundations. Stems were then grouted in place and branches trimmed to form typical classes of tree crowns, which can be seen in station photographs. Actual cutting was done 20 days before Shot 3. Trees were positioned at Stations I and II before Shot 2 and at Stations III and IV 10 days before Shot 3.

1/ Weighted disk on an aluminum beam.

Fig. 3.2 Station II Showing Lollipop and Trees A, B, C, and D (Left to Right) With Crowns 50, 60, 80, and 40 Per Cent of Total Height. View From Direction of Ground Zero.

Fig. 3.3 Station III Showing Lollipop and Trees A, B, C, and D (Left to Right) With Crowns 50, 50, 50, and 50 Per Cent of Total Height. View From Direction of Ground Zero.

Fig. 3.4 Station IV Showing Lollipop and Trees A, B, C, and D (Left to Right) With Crowns 50, 60, 80, and 40 Per Cent of Total Height. View From Direction of Ground Zero.

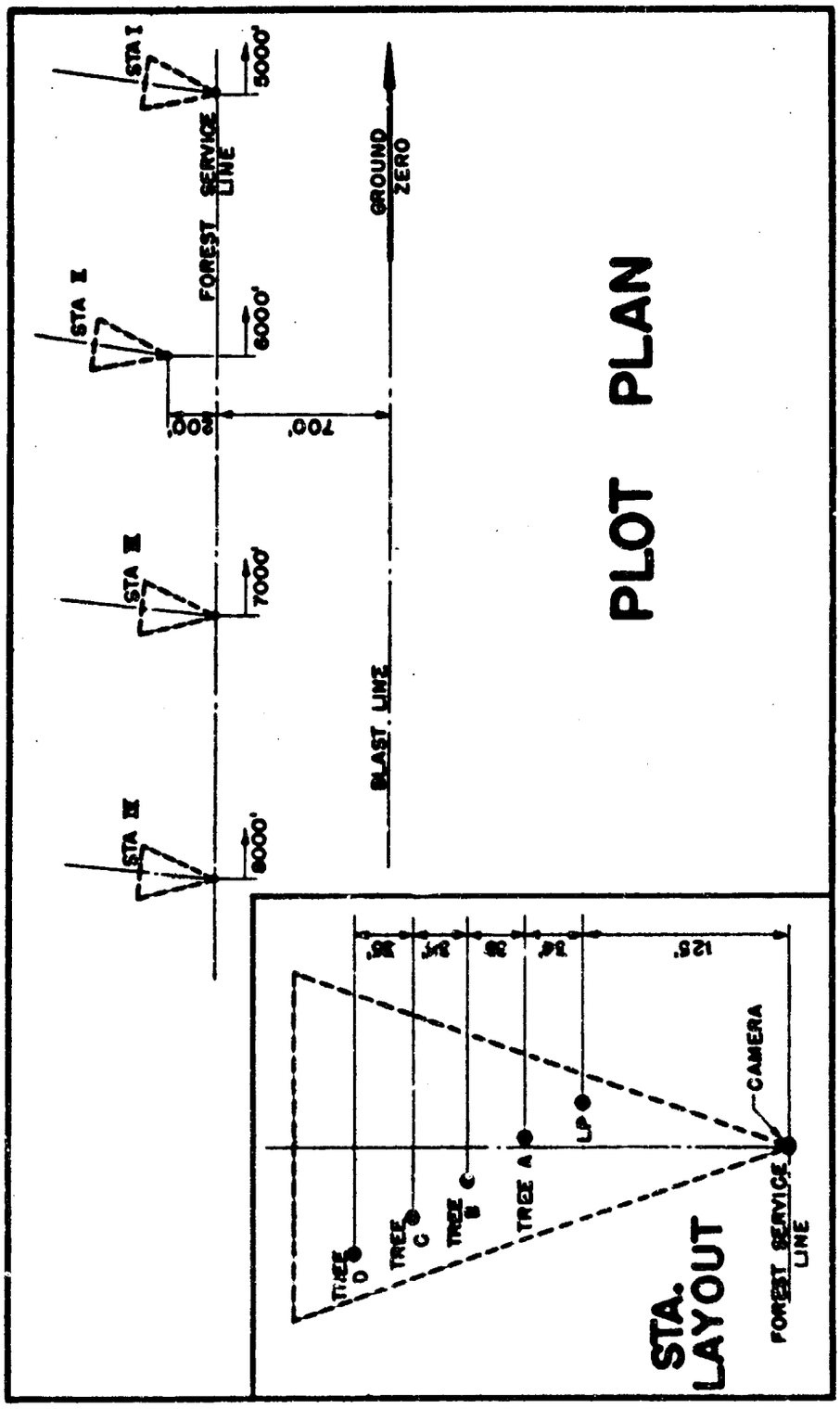

Fig. 3.5 Plot Plan and Station Layout

RESTRICTED DATA
ATOMIC ENERGY ACT 1946

Reference points were established on each tree stem at the center of the crown (which approximates center of pressure), and natural periods of vibration were measured prior to Shot 3.

Following each shot physical characteristics of broken trees were analyzed by measuring stem diameter inside bark at 5-ft intervals and by determining weight and moisture content of foliage and branchwood. After Shot 4, natural periods of standing trees were taken again. Static load-deflection and load-strain relations were then determined for "A" trees by pulling each tree with a cable attached to the stem at the reference point and measuring deflection, strain, and load until the tree broke. Physical characteristics of these and the remaining standing trees were then analyzed. These measurements and relations are summarized in Tables 3.1 and 3.2 and in Fig. 3.6.

TABLE 3.1

Mechanical Characteristics of Trees

Station and Tree	Deflection for Breakage* (Ft)	Spring Constant (Lb/Ft)		Strain Constant (μ In./In./Ft)	
		Reference Point	Center of Pressure	Reference Point	Center of Pressure
I A	15.0	146	237	627	672
II A	6.6	289	512	835	1250
III A	10.9	150	218	710	980
IV A	14.0	183	296	938	1280

* Deflection for breakage as a result of static loading applied at reference point.

RESTRICTED DATA
ATOMIC ENERGY ACT 1946

TABLE 3.2

Physical Characteristics of Trees

Station and Tree[a]	Stem Diameters			Height		Period	Tree Crown		
	DBH[b] (In.)	DIB[c] Ground Level (In.)	DIB Base of Crown (In.)	Total (Ft)	Reference Point[d] (Ft)	(Sec)	Nominal Per Cent of Tree Height	Length (Ft)	Dry Weight of Foliage and Branches (Lbs)
I A	10.7	9.4	5.2	34.2	26.2	1.38	40	13.6	80
I B	8.9	8.6	6.3	27.6	19.3	1.33	60	17.4	83
I C	10.5	10.0	9.0	35.9	21.9	1.28	80	29.2	200
I D	10.2	9.9	5.1	24.6	21.0	0.87	30	7.6	60
II A	10.7	10.3	6.7	34.2	25.9	1.04	50	17.2	88
II B	10.8	10.1	8.5	36.6	26.3	1.36	60	22.5	157
II C	10.5	10.2	9.1	27.9	18.0	1.13	80	24.0	145
II D	10.5	10.4	5.9	31.0	26.0	0.98	40	13.0	44
III A	10.7	9.8	7.0	38.9	28.0	1.48	60	24.0	90
III B	9.6	9.3	6.4	38.2	28.9	1.49	50	19.3	60
III C	7.5	7.1	5.0	32.6	25.1	1.31	50	16.8	23
III D	8.8	8.6	4.6	28.3	20.8	1.15	50	14.2	96
IV A	9.2	8.6	6.2	33.1	25.1	1.16	50	16.8	62
IV B	9.7	9.6	6.9	36.0	25.2	1.48	60	21.6	90
IV C	10.8	10.0	8.4	33.3	19.8	1.16	80	26.4	170
IV D	9.7	8.4	4.8	34.1	23.8	1.34	40	13.6	65

[a] All trees were western yellow pine, Pinus ponderosa var scopulorum Engelmann, except III D and IV C which were red fir, Abies magnifica Murray.

[b] Diameter at breast height, 4-1/2 ft above ground, outside bark.

[c] Diameter inside bark

[d] Height at which deflection measurements were made and static loads applied.

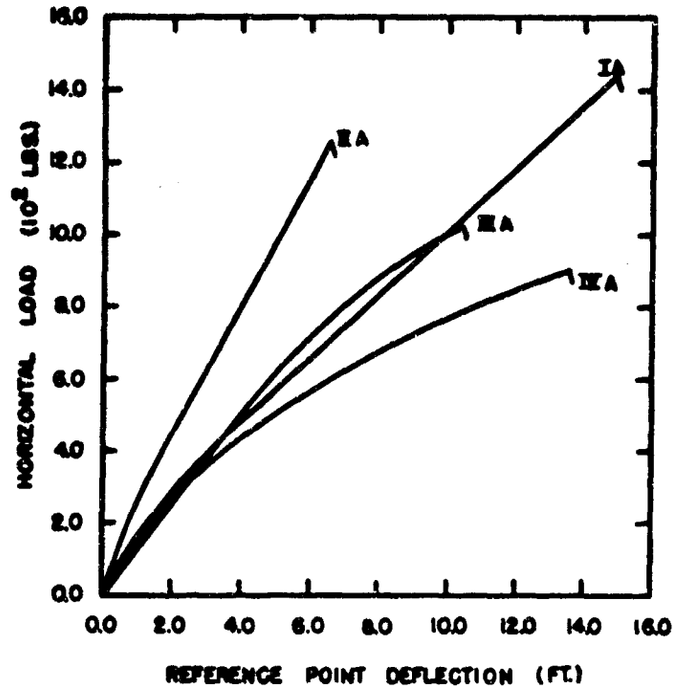

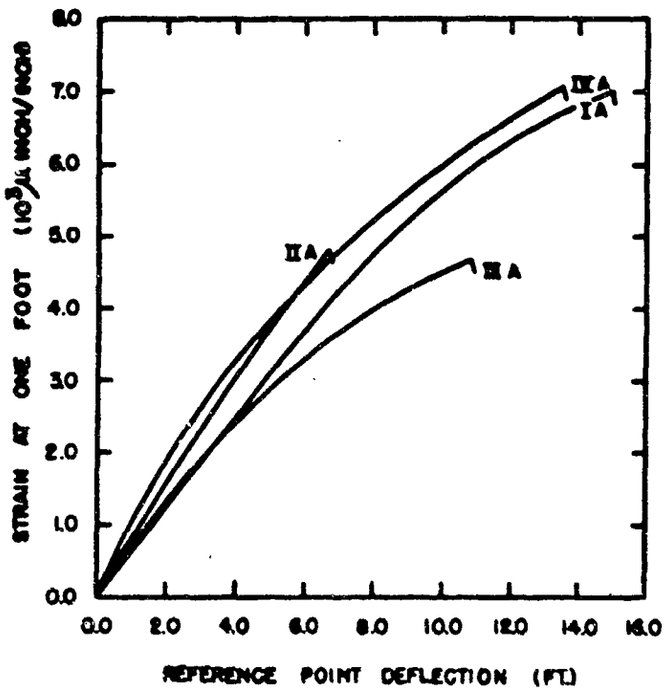

Fig. 3.6 Static Strain, Load, Deflection Relationships for Instrumented Trees

RESTRICTED DATA
ATOMIC ENERGY ACT 1946

3.2 LOLLIPOPS

A single-mass system was designed as an "ideal-reproducible tree" with a natural period typical of trees exposed. Natural period and other characteristics of the single mass system (Table 3.3) were reproduced in lollipops, which were constructed by mounting a 32-in. diameter steel, concrete-filled disk on an aluminum I-beam.2/

These I-beams were anchored in concrete foundations in the same manner as the trees and were guyed perpendicular to the radius from ground zero.

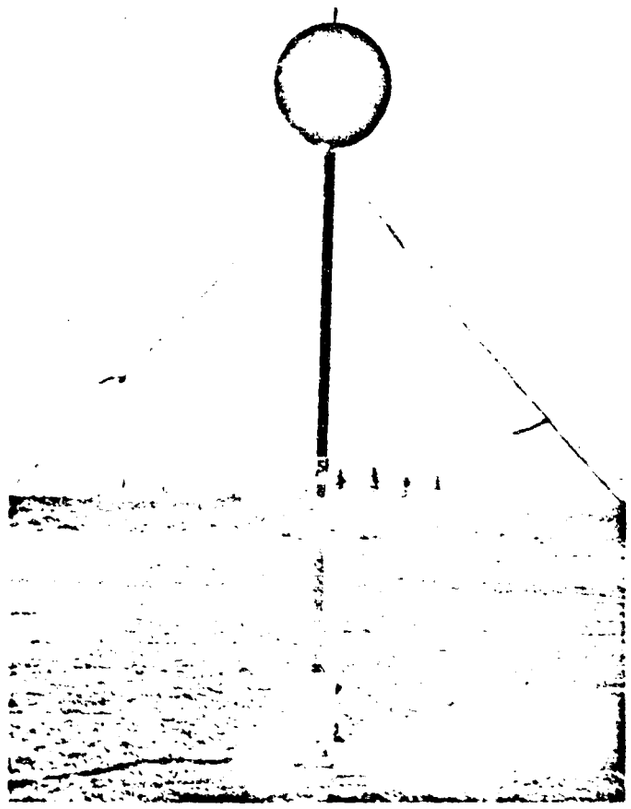

Fig. 3.7 Lollipop at Station I as Seen From Direction of Ground Zero. Steel Guard at Base Protects Strain Gage.

2/ 2.72-lb, 4-in. I-beam, alloy 61 ST 6.

TABLE 3.3

Lollipop Characteristics

Natural Period	-	1.18 sec	Spring Constant	-	341 lb/ft
Disk Weight	-	380 lbs	Disk Area	-	804 sq in.
Beam Weight	-	34 lbs	Beam Area	-	351 sq in.
Equivalent Total Disk Weight	-	387 lbs	Equivalent Total Disk Area	-	1005 sq in.
Strain Constant	-	1920 $\frac{\mu\text{in./in.}^{a}}{\text{ft}}$	Base Fixity[b]	-	0.75
Height to Center of Disk	-	14 ft			

[a] μin./in. = strain in microinches per inch
[b] Ratio of actual to theoretical spring constant values

3.3 INSTRUMENTATION

3.3.1 Strain-time Measurement

Baldwin SR-4 strain gages were mounted 7 in. above the base on the front and rear of each lollipop. A "strain meter" (Fig. 3.8) was mounted on the ground zero (tension) side of tree "A" at each station, 1 ft above the base, so that the gage could be affixed to the outermost wood surface (Fig. 3.9). Gage assemblies were protected from blast damage by foam rubber padding and steel guards similar to that shown in Fig. 3.7.

Strain meter and strain gage bridge output were recorded on Sanborn Model 127 oscillograph recorders equipped with Model 140 strain gage amplifiers. The system was independent of external power supply or timing signals. A block diagram of the power and relay system is shown in Fig. 3.10.

Power was supplied by four 12-volt, 50 amp. hr automotive wet batteries connected in series-parallel. Each oscillograph power circuit contained a separate 24- to 110-volt AC converter. Power consumption during the shot was only 4 amp. hrs so that battery voltage drop was small.

RESTRICTED DATA
ATOMIC ENERGY ACT 1946

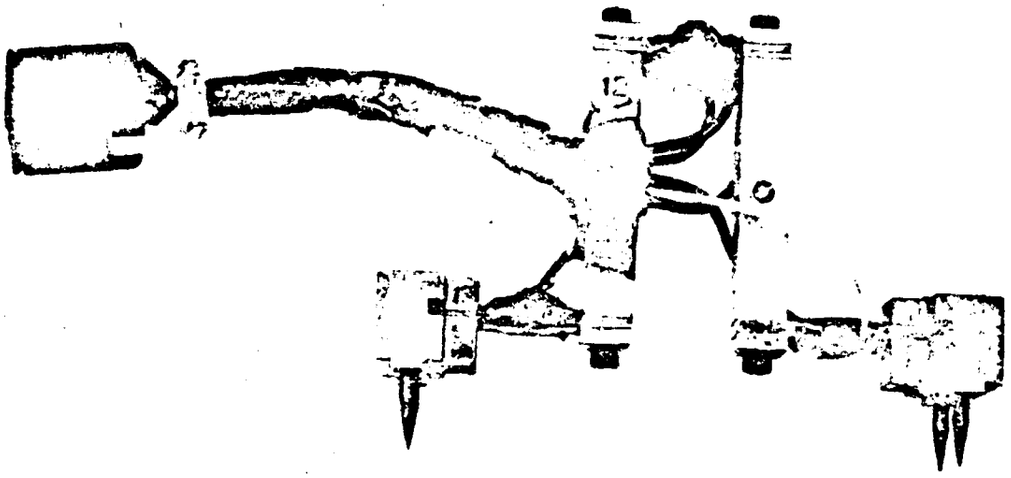

Fig. 3.8 Strain Meter

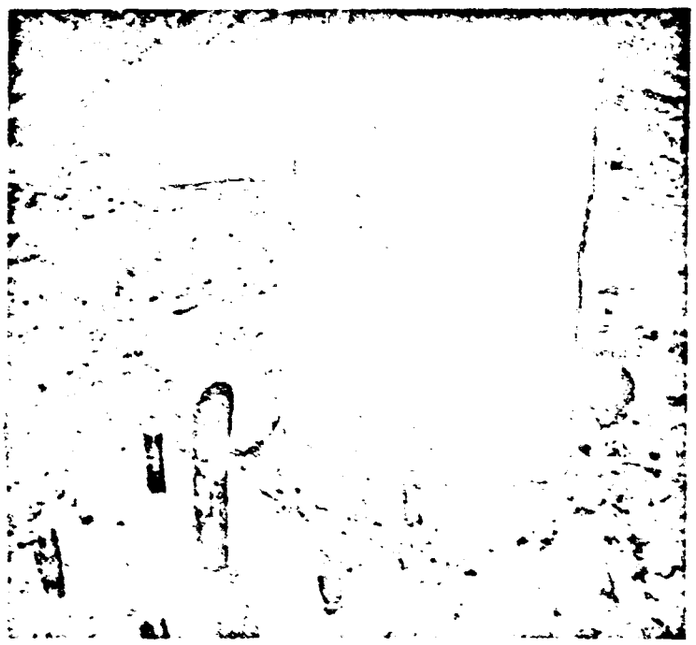

Fig. 3.9 Strain Meter Mounted on Tree

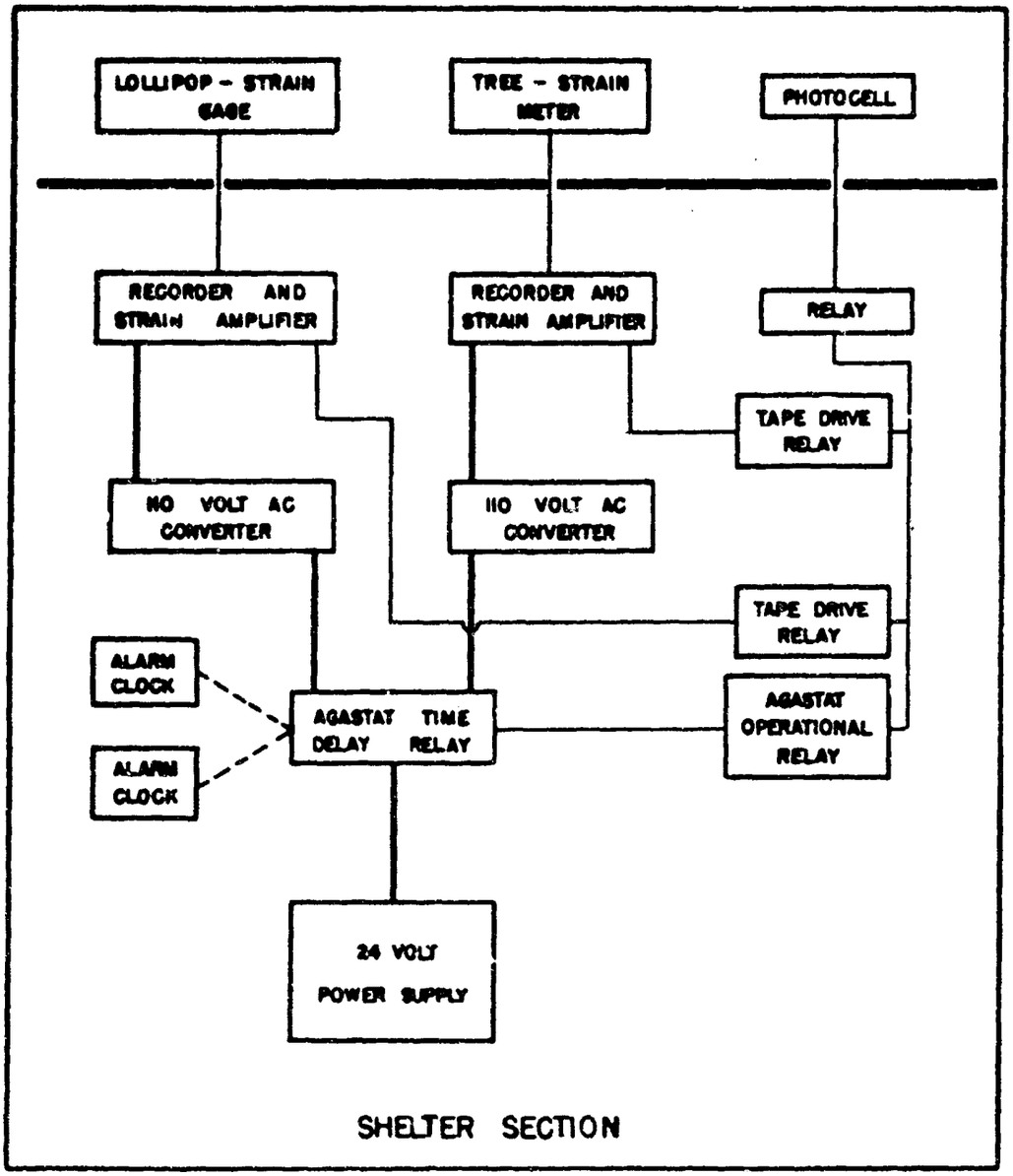

Fig. 3.10 Block Diagram — Oscillograph Power and Relay Systems

RESTRICTED DATA
ATOMIC ENERGY ACT 1946

All relays, except the photocell relay, were 24-volt aircraft mechanical-electrical latch in type as insurance against malfunction due to shock.

The two alarm clocks were set at H-10 hrs so that alarms would ring at H-1 hr and actuate the parallel toggle switches to close the Agastat circuit. Strain amplifiers were thus powered during a one-hour warm-up period for stabilization. The fireball tripped the photocell (Fig. 3.11), actuating the photocell relay, which in turn closed the two tape drive motor relays and opened the Agastat operational relay. After a time delay of 2 min., all power was turned off by the Agastat.

Fig. 3.11 Photocell and Mount Above Instrument Shelter

Upon recovery the toggles were opened and all relays were reset with an electrical reset switch. Alarms were reset and the system was immediately ready for operation.

The photcell circuit[3] was too sensitive. This defect was corrected by spraying the tubes with aluminum paint so that a Wabash Press No. 50 flash bulb would trip the relay at 2 ft but not at 10 ft.

All circuits leading to strain meters, strain gages, and photocells were shielded microphone cable. In addition, the first two cables ran through conduit providing magnetic as well as electrical shielding. All microphone cables and oscillographs were grounded to the conduit.

3/ Thomas I. Monahan et al. The Effect of Thermal Radiation on Materials. Naval Material Laboratory, New York Naval Shipyard. A.F.S.W.P. Report WT-311, Operation BUSTER, p. 26.

3.3.2 Maximum Strain Measurement

Baldwin deForest scratch gages were mounted to measure maximum strain at the following locations on trees:

1 ft above ground away from ground zero	- all trees
1 ft above ground toward ground zero	- trees B, C, D
Base of crown away from ground zero	- all trees

3.3.3 Maximum Deflection Measurement

Deflection snubbers were made by attaching piano wire to each tree at the reference point and to the center of the lollipop disk on the side towards ground zero. These wires led on a 45° angle to small snubbing blocks staked down on the ground zero side of the tree. Snubber wires were pulled tight and the length of long tails extending beyond the snubbers was measured prior to each shot. Snubber-wire ends were then remeasured upon recovery.

3.3.4 Motion Pictures

Camera stations for motion pictures were designed to place the plane of the film parallel to the radius from ground zero in order to measure deflection versus time. Figure 3.12 shows the camera view of tree movement. Also shown are aluminum foil bands which were placed on each tree 10 ft and 15 ft above ground level for scaling purposes. A foil band was also placed at the reference point. Thirty-five millimeter motion pictures were taken by the Army Pictorial Service Division, Office of the Chief Signal Officer, TUMBLER-SNAPPER Project 9.1.

Fig. 3.12 Station I Viewed From Motion Picture Camera Station

RESTRICTED DATA
ATOMIC ENERGY ACT 1946

CHAPTER 4

RESULTS

4.1 GENERAL

Overpressures and positive phase duration times to which trees and lollipops were exposed are shown in Table 4.1.

TABLE 4.1

Overpressures and Positive Phase Duration Times at Project 3.3 Stations, TUMBLER Shots 2, 3, and 4*

Station	Overpressure (PSI) 10-Ft Level				Positive Phase Duration Times (Sec) Ground Level		
	Peak			Incident			
	Shot 2	Shot 3	Shot 4	Shot 3	Shot 2	Shot 3	Shot 4
I	1.3	5.3	4.1	2.1	0.42	0.98	0.98
II	1.0	4.3	2.9	1.6	0.43	1.02	1.02
III	-	3.6	2.2	-	-	1.06	1.05
IV	-	3.6	1.8	-	-	1.09	1.09

* Interpolated from data furnished by the Armed Forces Special Weapons Project. 9 May 1952

Six trees were broken on Shot 3, and one of the remaining trees on Shot 4 as shown in Table 4.2. No main branches were broken by either blast. There were a few scattered twigs on the ground at each station after Shot 3 but none after Shot 4.

Unbroken trees and lollipops did not appear to be damaged structurally. Strain and deflection calibrations and natural period measurements made before Shot 3 and after Shot 4 agreed within limits of experimental error.

TABLE 4.2

Characteristics and Circumstances of Tree Breakage

Station and Tree	Shot	Over-pressure* (PSI)	Height of Break Above Base (Ft)	Type of Break
I C	3	5.3	1	Diagonal bending failure
I D	3	5.3	14	Diagonal bending failure originating at knot on tension
II B	3	4.3	2	Short bending failure
II C	3	4.3	9	Brash failure at knot cluster
II D	3	4.3	19	Brash failure at one knot on tension
III D	3	3.6	13	Diagonal tension failure
I B	4	4.1	7	Diagonal tension failure

* Ten-ft-level values, se Table 4.1.

Fig. 4.1 Breakage of Trees B, C, D at Station II, Shot 3

RESTRICTED DATA
ATOMIC ENERGY ACT 1946

A B

Fig. 4.2 Typical Stem Failures. A - Brash Failure at One Knot on Tension; Tree II D. B - Diagonal Tension Failure; Tree III D.

Tree breakage and non-breakage data for Shots 3 and 4, Figs. 4.3 and 4.4, were normalized in the manner described in Appendix A. Dynamic pressure ratio was used rather than shock-pressure ratio because the former is compatible with both regular and Mach reflection types of shock when loading is principally due to drag. Dynamic pressures for breakage due to steady wind were estimated from tree characteristics given in Table 3.2. Conditional breakage regions in Figs. 4.3 and 4.4 correspond to that predicted theoretically (Fig. 2.2) when it was moved parallel to itself so that it separated non-breakage and breakage data. No weight was given to the three trees which failed at knots and which consequently fell in the region of non-breakage in Fig. 4.3.

4.2 DEFLECTION, TIME HISTORY — TREES

Deflection-time histories and maximum deflections were scaled from motion pictures whenever clarity permitted. Since a comparison of motion picture time of shock arrival with actual shock arrival times

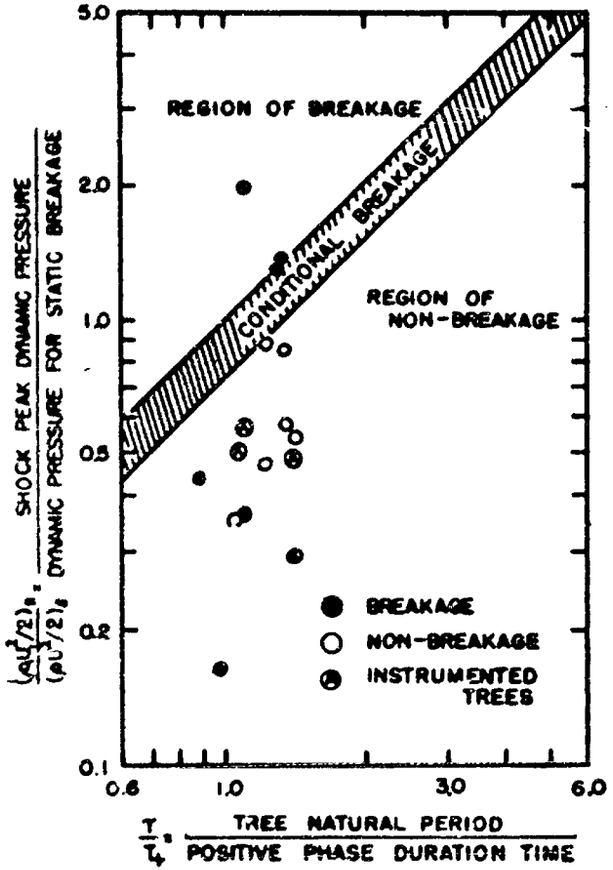

Fig. 4.3 Regions of Breakage and Non-Breakage—Conifers, Shot 3

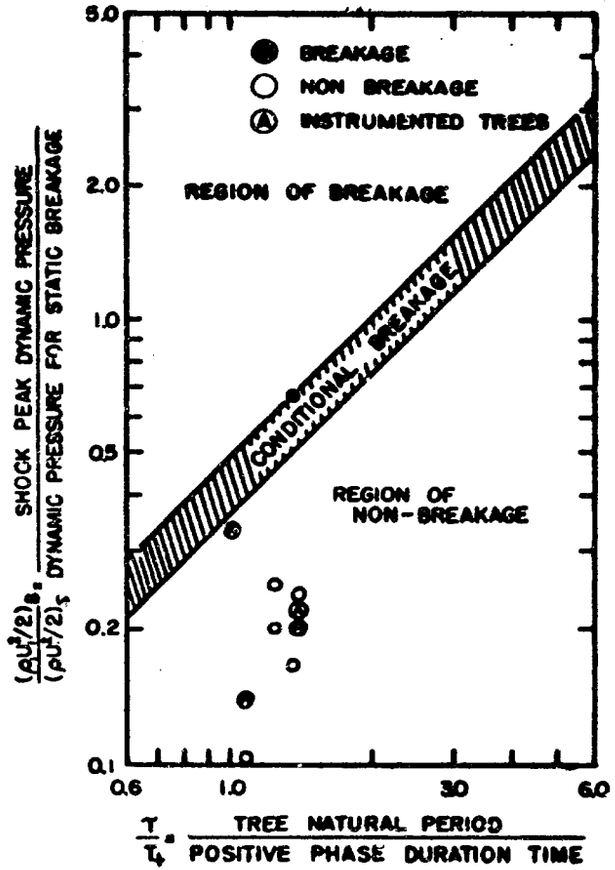

Fig. 4.4 Regions of Breakage and Non-Breakage—Conifers, Shot 4

Dynamic Pressure for Static Breakage is Based on Velocity and Density Associated With Breakage Due to Steady Wind

showed wide variation from nominal film speed of 64 frames/sec, film speed was estimated from oscillograph records of instrumented trees, Table 4.3. Oscillograph tape speed timed before and after each shot showed a maximum disparity of 8 per cent.

TABLE 4.3

Oscillograph Time of Arrival and Film Speed Data

Shot	Station	Time of Shock Arrival[a] (Sec)	Oscillograph Time of Arrival[b] (Sec)		Film Speed (Frame/Sec) Based On	
			Trees	Lollipops	Time of Shock Arrival	Oscillograph Tape Speed[c]
2	I	3.90	3.73	3.77	41.3	
3	I	3.84	3.68	3.62	53.4	-
	II	4.55	4.56	4.51	57.2	54.7
	III	5.28	5.42	5.22	57.5	-
	IV	5.93	5.85	6.13	84.5	60.8
4	I	2.96	2.80	2.81	29.1	31.8
	II	3.78	3.68	3.64	62.4	64.6
	III	4.57	4.51	4.48	64.3	64.6
	IV	5.38	5.37	4.87	76.4	73.5

[a] Interpolated from data furnished by the Armed Forces Special Weapons Project. 9 May 1952

[b] Not to be taken as true times of arrival — for comparison only.

[c] During time of tree motion.

Deflection-time histories and maximum deflections were determined from strain meter data (Fig. 4.5) by dividing measured strain at 1 ft by the static strain constant for the reference point.

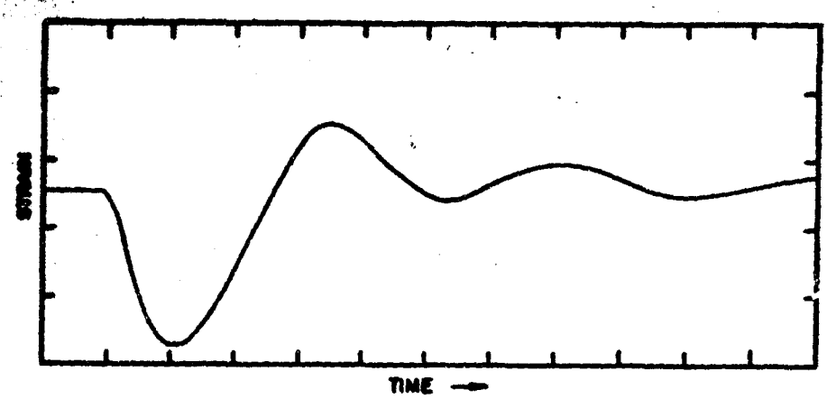

Fig. 4.5 Tracing of Strain Meter Record, Tree I A, Shot 3. Strain = 1090 μ in./in./division; Time = 2.68 division/sec.

Deflection-time histories computed by the method described in Section 2.2 are compared with those scaled from motion pictures and those determined from strain meter data in Figs. 4.6, 4.7, and 4.8. Maximum deflection data are compared in Table 4.4.

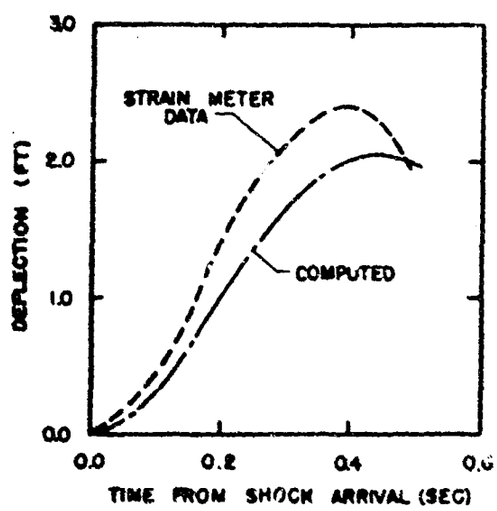

Fig. 4.6 Motion of Reference Point Under Blast Loading, Tree I A, Shot 2

RESTRICTED DATA
ATOMIC ENERGY ACT 1946

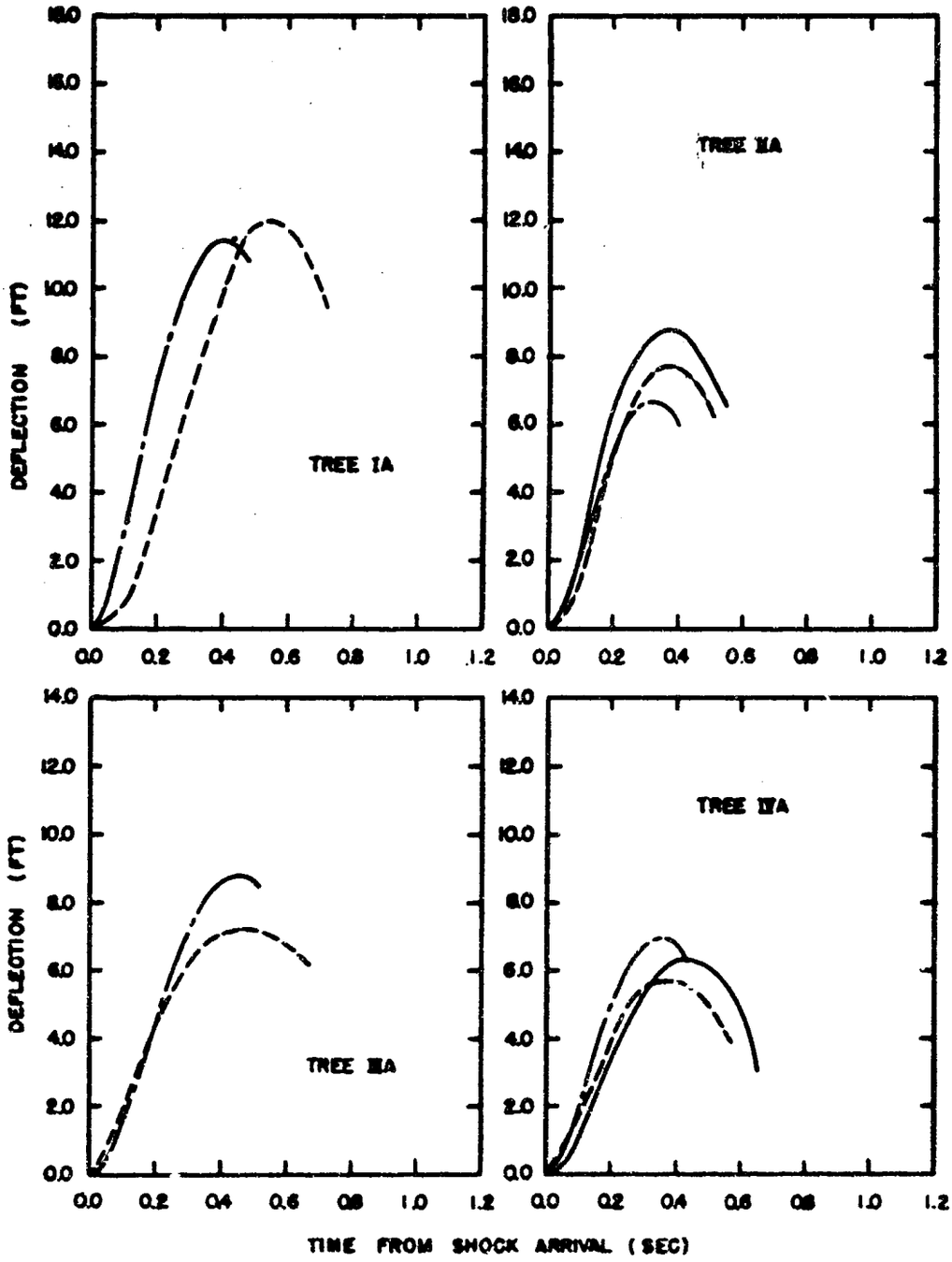

Fig. 4.7 Motion of Reference Point Under Blast Loading—Trees, Shot 3. See Table 3.2 for Reference Point Height.

——— Motion Picture Data
– – – – Strain Meter Data
—·— Calculated

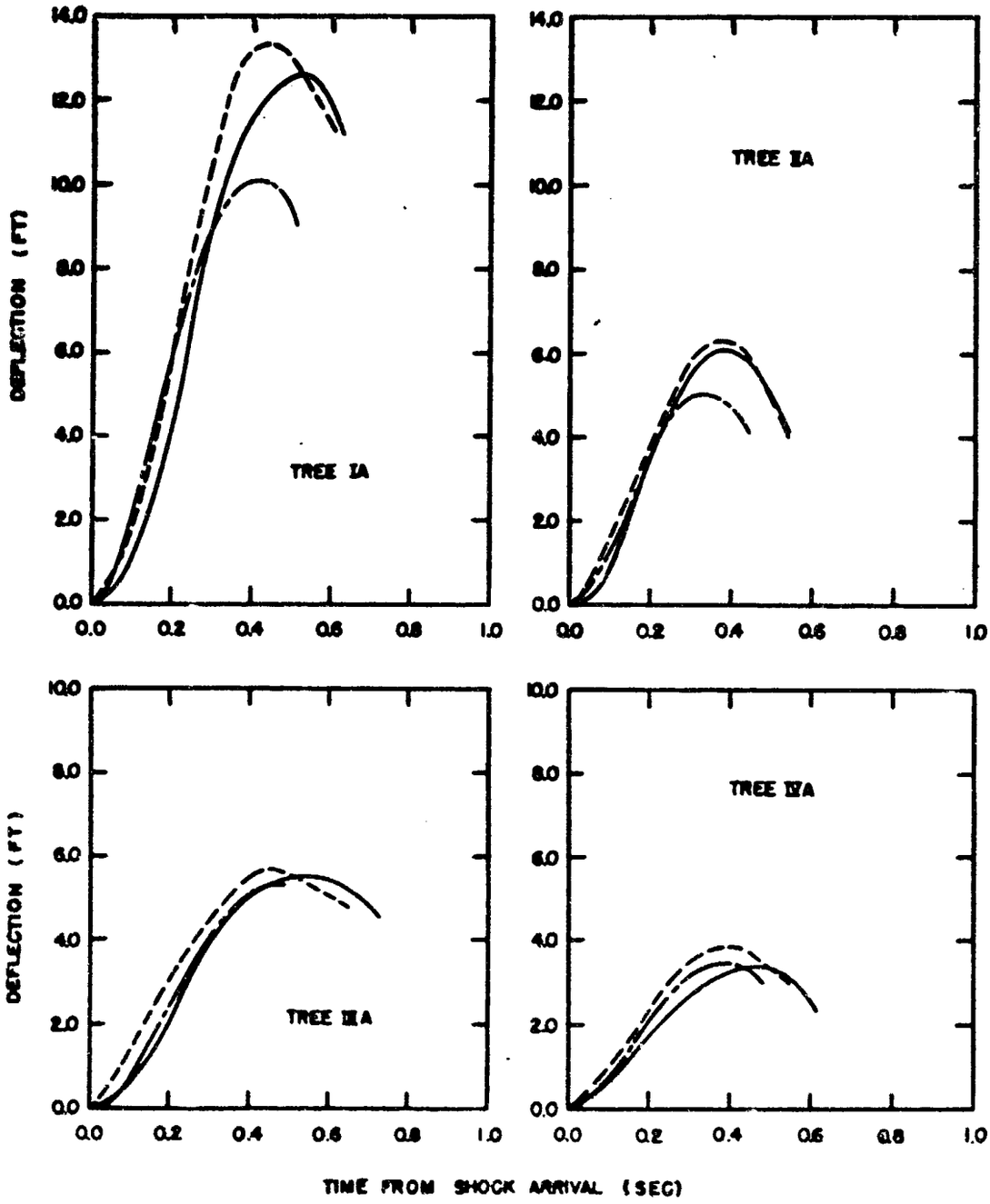

Fig. 4.8 Motion of Reference Point Under Blast Loading—Trees, Shot 4. See Table 3.2 for Reference Point Height.

——— Motion Picture Data
- - - - - Strain Meter Data
—·— Calculated

RESTRICTED DATA
ATOMIC ENERGY ACT 1946

CONFIDENTIAL
Security Information

TABLE 4.4

Maximum Tree Deflections

Station and Tree	Height of Reference Point (Ft)	Maximum Deflection of Reference Point (Ft)									
		Shot 2		Shot 3				Shot 4			
		Strain Meter[a]	Calculated	Snubber	Motion Picture	Strain Meter	Calculated	Snubber	Motion Picture	Strain Meter	Calculated
I A	26.2	2.4	2.1	10.2	-	12.0	11.5	10.7	12.7	13.3	10.3
I B	19.3			8.4	-			B[b]	9.2[c]		
I C	21.9			B	-				-		
I D	21.0			B	-				-		
II A	25.9			15.1[d]	8.8	7.7	6.7	6.0	6.1	6.4	5.0
II B	26.3			B	-				-		
II C	18.0			B	-				-		
II D	26.0			B	-				-		
III A	28.0			14.6[d]	-	7.2	8.9	5.7	5.5	5.7	5.3
III B	28.9			8.2	-			6.8	5.9		
III C	25.1			10.1	-			5.5	5.6		
III D	20.8			B	-				-		
IV A	25.1			5.3	6.3	5.7	7.0	3.3	3.4	3.9	3.5
IV B	25.2			5.4	6.8			4.0	5.1		
IV C	19.8			3.0	-			2.0	2.4		
IV D	27.2			5.9	-			3.4	3.9		

[a] Measured strain at 1 ft divided by static strain constant for reference point.
[b] B = Tree broken. [c] Deflection for breakage [d] Questionable--snubber wire moved.

CONFIDENTIAL
Security Information
RESTRICTED DATA
ATOMIC ENERGY ACT 1946

4.3 MAXIMUM DEFLECTION — LOLLIPOPS

Maximum deflections were measured from motion picture films, but relative movements of lollipop centers of pressure were too small for measurement of deflection-time histories. Oscillograph data were processed in the same manner as tree strain meter data. Maximum deflections for centers of pressure are shown in Table 4.5 and are compared on a dimensionless basis in Fig. 4.9.

TABLE 4.5

Maximum Lollipop Deflections

Shot	Station	Maximum Deflection (Ft)			Time to Max. Deflection (Sec)	Peak Dynamic Pressure (PSI)
		Oscillograph	Snubber	Movies		
2	I	0.0995	-	-	0.30	0.052
3	I	T*	1.73	-	-	0.55
	II	1.16(T)	1.52	1.48	0.46	0.41
	III	1.10	1.09	-	0.39	0.35
	IV	1.13	0.97	0.85	0.42	0.35
4	I	T	2.03	2.16	-	0.42
	II	0.868(T)	1.02	1.15	0.44	0.24
	III	0.578	0.64	0.54	0.40	0.15
	IV	0.605	0.52	0.48	0.39	0.098

* T — data not reliable due to twisting of lollipop

4.4 SCRATCH GAGE STRAIN MEASUREMENT

Maximum strain values in Table 4.6 were read with a toolmaker's microscope to the nearest 0.0002 in. (equivalent to a strain of 0.1 μ in./in.) directly from scratch gage targets. Figure 4.10 presents a typical target record. Only 6 out of 70 gages failed to record.

Data from simultaneous free vibration records taken on Tree IV A with scratch gage and strain meter on opposite sides of the stem are compared in Fig. 4.11.

RESTRICTED DATA
ATOMIC ENERGY ACT 1946

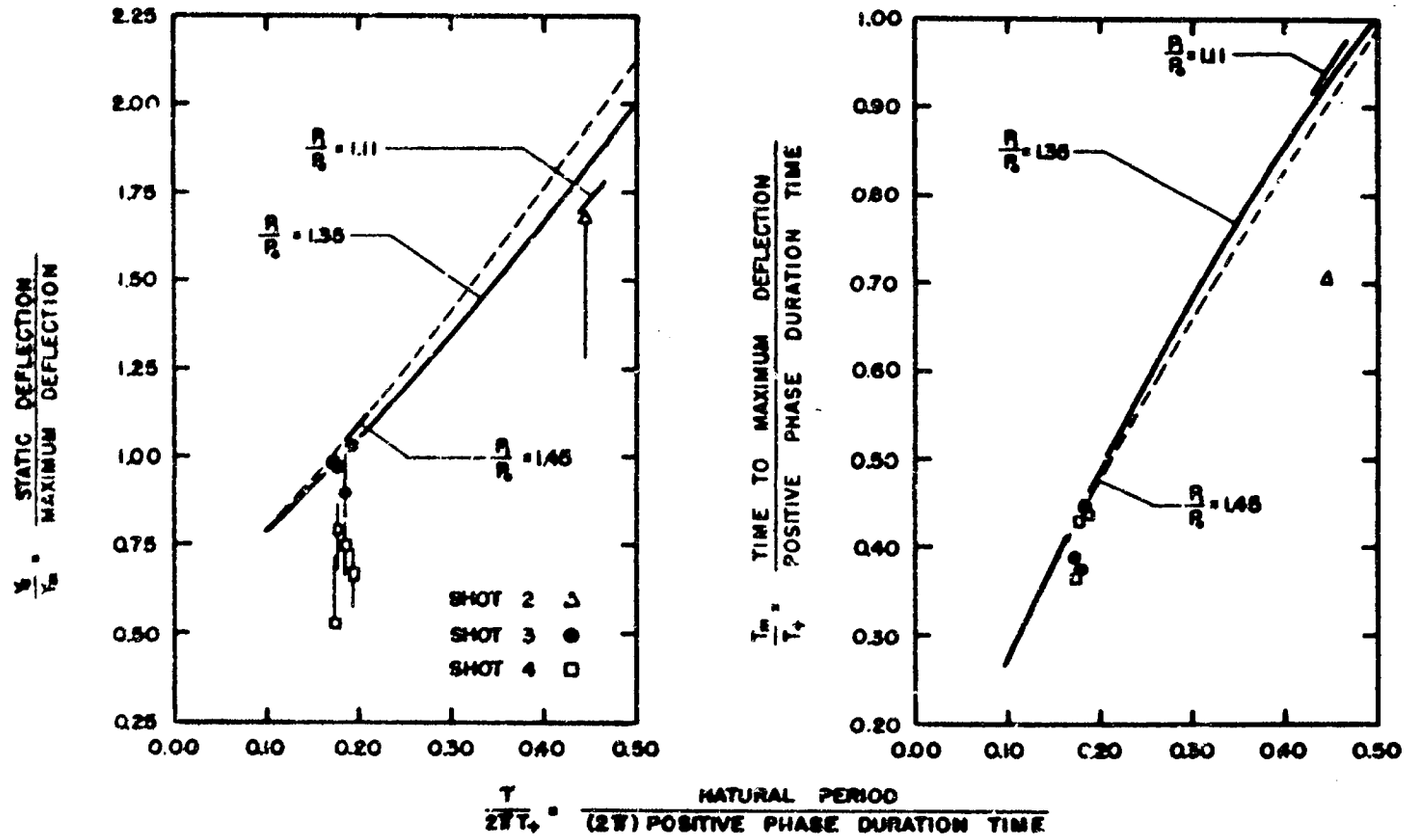

Fig. 4.9 Normalized Lollipop Maximum Deflection and Time to Maximum Deflection, Shots 2, 3, and 4. Static Deflection is the Deflection Under Static Loading Associated With Shock Peak Dynamic Pressure. Solid Lines Represent Theory Based on Free Air Density and Velocity Decay for Different Shock Pressure Ratios. Dashed Lines Represent Theory for Linear Decay. Vertical Lines Through Data Points Indicate Maximum Spread of Data.

RESTRICTED DATA
ATOMIC ENERGY ACT 1946

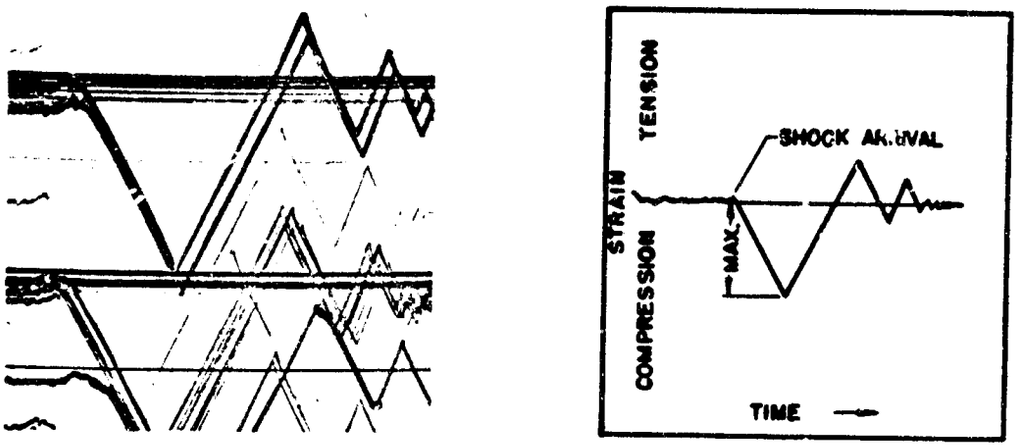

Fig. 4.10 Scratch Gage Record and Diagrammatic Explanation (Magnification = X 32). Tree IV B, Shot 3, 1 Ft Above Ground Away From Ground Zero.

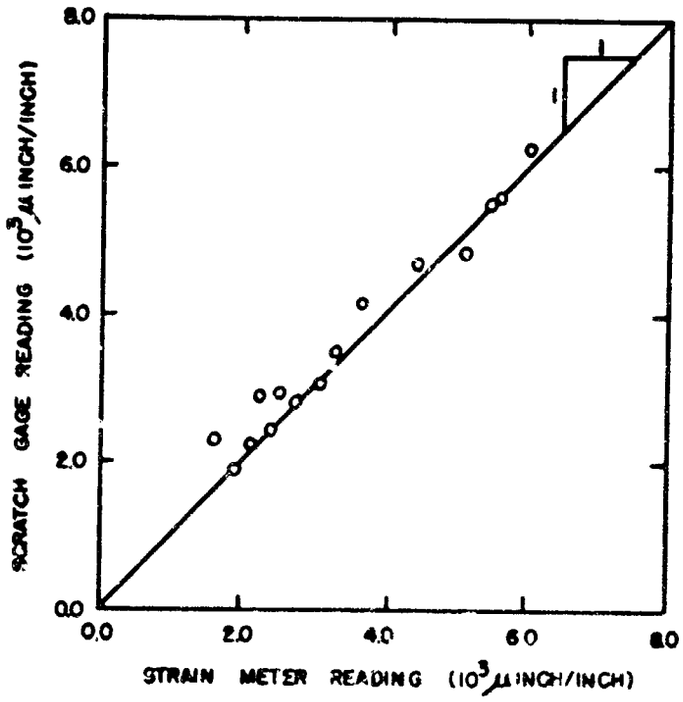

Fig. 4.11 Comparison of Strain Measurement — Scratch Gage Versus Strain Meter

RESTRICTED DATA
ATOMIC ENERGY ACT 1946

TABLE 4.6

Maximum Strain Comparison — Scratch Gages and Strain Meters, TUMBLER-SNAPPER Shots 3 and 4

Station and Tree	Shot 3 Maximum Strain, 10^3 μ in./in.			Shot 4 Maximum Strain, 10^3 μ in./in.		
	F-1[a]	R-1[a]	R-C[a]	F-1	R-1	R-C
I A	7.55[b]	17.5	21	8.33	21.4	17.3
I B	8.4	14.5	32.5	17.4	19.3	33.3
I C	5.2	U[c]	11.6	M[d]	M	M
I D	U	8.5	7.9	M	M	M
II A	6.40	8.6	10.3	5.25	7.9	9.1
II B	B[e]	U	10.9	M	M	M
II C	B	12.6	12.9	M	M	M
II D	U	5.9	12.7	M	M	M
III A	5.08	4.3	9.8	4.00	5.7	8.0
III B	5.0	8.9	8.4	3.5	6.5	7.1
III C	U	8.4	5.5	3.6	4.9	4.4
III D	7.6	11.8	15	M	M	M
IV A	5.35	6.2	6.2	3.62	4.4	5.7
IV B	5.6	5.2	8.0	3.5	3.8	3.6
IV C	5.7	6.4	5.0	2.6	3.3	2.9
IV D	6.9	U	5.3	2.3	3.7	4.0

[a] Gage location on tree:
F-1, tension, 1 ft above ground facing ground zero
R-1, compression, 1 ft above ground facing away from ground zero
R-C, compression, at base of crown facing away from ground zero

[b] Underlined values recorded by strain meter located in F-1 position

[c] U = Record unreadable or missing

[d] M = No record; tree broken by Shot 3

[e] B = No record; tree break near gage

CHAPTER 5

DISCUSSION

5.1 GENERAL

Predictions of minimum overpressures which will break forest trees are based on calculations which assume that stem loading is the result of aerodynamic drag of the tree crown due to after-shock winds. Aerodynamic drag characteristics of crowns have been determined experimentally and correlated on a dimensionless basis with physical crown characteristics. Calculations to date have been based on linear time variation of after-shock particle velocity and density or on the theoretical time history appropriate to free air as shown in Fig. A.2. However, the validity of applying free air time histories in regions of regular and Mach reflection remains to be verified.

5.1.1 Correlation of Shot 3 Lollipop Data

Maximum particle velocity and density following shock — peak dynamic pressure — determines the magnitude of forces acting on trees. In the Mach reflection region peak dynamic pressure was calculated from peak overpressure by normal shock equations; in the region of regular reflection the calculation was based on incident and reflected shock overpressures by using oblique shock equations. Resultant peak dynamic pressure values are shown in Table 4.5 and correlated lollipop deflection data for Shot 3 are shown in Fig. 4.9.

If the fact that Stations I and II were in the regular reflection region on Shot 3[1] (Stations III and IV were in the Mach reflection region) is neglected and peak dynamic pressure at those two stations is computed by normal shock equations, this failure to account for oblique shock produces a 35 per cent discrepancy between correlated lollipop deflections at the first two stations and the last two stations.

These correlation studies indicate that peak dynamic pressure and duration time are the fundamental shock parameters for predicting or comparing damages to structures such as trees, suspension bridges and towers, which have comparatively long periods and are affected primarily by aerodynamic drag. These parameters are particularly applicable for damage comparison between regular and Mach reflection regions.

1/ Test Data Furnished by the Armed Forces Special Weapons Project. 15 May 1952.

5.1.2 Comparison of Shot 3 and Shot 4 Results

Differences between results of Shot 3 and Shot 4 are summarized below:

1. Lollipop maximum deflections at Station I were higher on Shot 4 than on Shot 3 even though peak dynamic pressure determined from reported overpressures for Shot 4 was less than for Shot 3, and the positive phase duration times were the same (Tables 4.1 and 4.5).

2. Lollipop maximum deflections for all stations on Shot 4 were higher than predicted when this prediction was based on results of Shot 3 and overpressures as reported for Shot 4.

3. Maximum deflection from snubber data and maximum base strain from strain meter and scratch gage data for tree I A, Shot 4, were higher than for Shot 3.

4. Tree I B, unbroken on Shot 3, was broken on Shot 4. This tree appeared structurally and physically unchanged after Shot 3.

These differences indicate that results from Shots 3 and 4 could not be correlated satisfactorily even though allowance was made for Mach and regular reflection occurrence as discussed in the previous section. The only area of agreement between Shots 3 and 4 lies in the time to maximum deflection for the lollipops. Little doubt remains, however, that higher comparative deflections of Shot 4 over Shot 3 were a true phenomenon. These data tend to support the hypothesis that factors heretofore not considered caused peak dynamic pressures on Shot 4 to be higher than indicated by reported peak overpressures.

Sandia Laboratory pitot tube results[2/] lend supporting evidence to the above hypothesis. Measured dynamic pressures on Shot 4 at the 13-ft level were 20 to 30 per cent higher than those computed from measured overpressures in the 3 to 8 psi overpressure region. Measured Shot 3 dynamic pressures were in substantial agreement with computed values. Further, but inconclusive, support originates in Los Alamos Scientific Laboratory Shot 4 smoke velocity data.[3/] Measurements at the 300-ft level indicate peak particle velocities 10 to 15 per cent higher than those calculated from overpressure measurements made nearer the ground.

2/ Sandia Laboratory. Shock-Gauge Evaluation Tests. A.F.S.W.P. Operation TUMBLER-SNAPPER Report WT-505, Projects 19.1c and 19.1d.
3/ Verbal communication with F. B. Porzel of Los Alamos Scientific Laboratory, September 17, 1952.

Both data are subject to scatter due to low resolution at low overpressure level; however, they agree in order of magnitude and indicate the possibility of a 30 per cent increase in dynamic pressure over computed values. A 30 per cent correction added to dynamic pressures used for correlation of Shot 4 lollipop deflection and tree breakage data would bring them into juxtaposition with Shot 3 data.

An additional pressure pulse occurred on Shot 4 during the positive phase.4/ Since this occurred after maximum displacements of lollipops and trees it may be presumed that this secondary shock had no effect on these displacements.

5.2 TREE BREAKAGE

Due to the limited number of tree installations and to the fact that no two trees are exactly alike, prediction of tree breakage must lean heavily on calculation procedures and extrapolation of data by theoretical means. In addition, because of the reduction of KT on Shot 3 from the originally intended bomb size, none of the fully instrumented trees broke. These situations precluded full exploitation of the theory of breakage developed in Chapter 2; however, breakage, nonbreakage, and conditional breakage regions of Figs. 4.3 and 4.4 have been defined. Results of Shots 3 and 4 are displayed separately since the discussion in Section 5.1.2 indicated shock phenomena were different in each case.

The conditional breakage region determined from theoretical considerations alone (Fig. 2.2) is subject to certain inherent inaccuracies in magnitude. Although the equation of motion may be integrated with sufficient accuracy, dynamic breakage deflections are in doubt due to a lack of complete knowledge of the increase in strength of green timber under high loading rates. Further, more recent static breakage data indicate that approximately 50 per cent of all trees will be stronger than the trees used as the basis of the conditional breakage region displayed in Fig. 2.2. The procedure followed in the theoretical analysis should produce the correct variation with respect to period ratio; however, dynamic pressure magnitudes must be adjusted in accord with field experiments as was done in Figs. 4.3 and 4.4.

Considerable scatter is inherent in such plots as Fig. 4.3 and 4.4 because of variations in tree characteristics and because it is unlikely that a tree is located just at the breaking point on any one

4/ U. S. Naval Ordnance Laboratory. Free Air and Ground Level Pressure Measurements. A.F.S.W.P. Operation TUMBLER Report, Projects 1.3 - 1.5. 15 September 1952.

shot. However, it is believed that the three breakage points on Shot 3 which fall within the region of non-breakage (Trees I D, II C, II D) are not chance variations since these and only these trees broke at knots as shown in Table 4.2. It is possible that stress concentrations occur at certain knot combinations. More actual breakage data for static and dynamic loading are needed to establish the validity of this hypothesis.

In Figs. 4.3 and 4.4 conditional breakage regions were located to separate breakage and non-breakage data except for the case described above. The scatter in these diagrams as well as the Shot 3 variations indicate need for more test data which, added to that already obtained, can be used to establish breakage probabilities associated with variations in tree and shock parameters.

Section 5.1.2 and the above discussion indicate that the conditional breakage region determined from Shot 3 data (Fig. 4.3) represents the better basis for the lower limit of dynamic pressure approaching complete breakage of isolated conifers.

The combination of tree periods and positive phase times of Shots 3 and 4 grouped data at the lower end of the period ratio scale (Figs. 4.3 and 4.4). Since periods of growing trees of the type used for Operation SNAPPER range from 2 to 4 sec and periods of some species range up to 14 sec, future tests should cover a greater range of period ratio. With improved methods of installation it may be possible to increase tree periods to 2 sec; however, an increase in range of positive phase duration times as well as overpressure should also be provided through variations in bomb size.

Stem breakage occurred near the base of the crown or below, and in no case did the crown break up. However, since these trees were selected because they had no defect and no dead limbs, breaks at such defective points in stems and crowns can be anticipated in a natural forest.

5.3 DEFLECTION-TIME HISTORY — TREES

Deflection-time data determined from strain measurements generally agreed with those determined from motion pictures when strain constant at small deflection was used. However, had the full static strain-deflection curve (Fig. 3.6) been used, excessive deflection values would have been obtained from strain meter data, and in some cases such deflection determinations would have been in excess of breakage.

It has been established[5] that under conditions of high loading rate, the yield point for wood increases above its static value. Sufficient data are not available in the literature to predict this increase for growing trees. Project 3.3 results indicate that this increase for green timber is much greater than would be predicted from dry wood data. One example is found in the fact that Tree II A failed under static loading at a deflection of 6.6 ft, while motion pictures showed its deflection on Shot 3 to be 8.8 ft without breaking. This phenomenon cannot be explained by moisture content difference after Shot 3 (90 per cent) and after Shot 4 (60 per cent), because within this range experimental evidence indicates that there is no appreciable change in the static strength of wood.

A detailed examination of corresponding motion picture deflections and strain meter readings should lead to the determination of the stress-strain relationship under dynamic loading. Unfortunately this comparison cannot be made in the region close to breakage, since none of the instrumented trees failed. Furthermore, film speed of the motion pictures was in doubt. Consequently, film speed was arbitrarily made to agree with oscillograph tape speed by matching times at initial and first zero deflection positions. Agreement or disagreement between times to maximum deflection is coincidental.

As a result of the high yield point when loading rate is high, deflection calculations on instrumented trees were made using the linear load-deflection relationship as determined from the spring constant instead of using the static load-deflection relationship described in Section 3.1. Had the latter method been used, greater deflections would have been calculated, and in some cases breakage would have been predicted.

Drag determinations were made from previous work[6] which established weight ratio of foliage to branch wood and crown weight as the most important tree parameters affecting drag. Since SNAPPER test trees were cut prior to the current year's needle growth, the weight ratio based on these previous studies, which were made in late summer when needle growth was complete, was reduced by one-third.

Calculated maximum deflections were within 20 per cent of measured values. Agreement among calculated deflection-time histories is considered good in view of the number of variables involved. This agreement substantiates use of the single mass approximation used in previous conifer analyses and use of the free air time dependency of particle velocity and density as a suitable approximation in the regular reflection and Mach stem regions.

5/ L.J. Marquardt and T.R.C. Wilson. Strength and Related Properties of Woods Grown in the United States. U. S. Dept. of Agriculture Tech. Bul. 479, Washington: U.S. Govt. Printing Office, 1935. p. 60.
6/ Forest Service, Aerodynamic Drag in Tree Crowns, op. cit.

5.4 DEFLECTION-TIME HISTORY — LOLLIPOPS

Derivation of the equation of motion outlined in Appendix A indicates that normalized maximum deflection is a function of four dimensionless variables for any particular particle velocity and density history.

$$\frac{Y_m}{Y_s} = f\left(\frac{\mathcal{T}}{2\pi T_+}, \frac{Y_s}{U_1 T_+}, \frac{Y_s}{L}, \frac{P_1}{P_o}\right)$$

Prior to TUMBLER-SNAPPER a series of numerical integrations was performed using a linear time dependency for particle velocity and density. These calculations covered the range of variables expected for the lollipops during the test as shown in Table 5.1.

TABLE 5.1

Range of Variables Covered by Deflection Calculations

	$\frac{\mathcal{T}}{2\pi T_+}$	$\frac{Y_s}{U_1 T_+}$	$\frac{Y_s}{L}$	$\frac{P_1}{P_o}$
Minimum	0.1	0.0025	0.00175	1.11
Maximum	0.5	0.0050	0.10	1.45

In the range indicated above only the period ratio was significant, shock overpressure was second order, and the remaining two variables insignificant. TUMBLER lollipop data remained within the above range of calculations.

A second set of integrations was performed using free air decay of particle velocity and density shown in Fig. A.2 for mean values of Y_s/U_1T_+ and Y_s/L and pressure ratio range experienced at TUMBLER.

Figure 4.9 compares results of these two computations. Use of linear decay gives somewhat higher deflection ratios at higher period ratio, but the disparity is not great.

Maximum deflection and time to reach maximum deflection data were normalized as described above. Points plotted in Fig. 4.9 are based on averages of the three methods of measuring deflection except at closer stations, where twisting of lollipop beams invalidated strain gage records. In these cases motion picture and snubber data were used to calculate plotted points.

Shot 4 data fall below the predicted curve for reasons discussed previously. Since the strain record went off scale on the one Shot 2 record, estimated maximum strain and the resultant plotted point may be unreliable. Shot 3 results are considered to be the most reliable, and agreement between these experimental points and theory is good.

Substantiation of the calculation method by these lollipop data and the close approximation of the linear velocity decay calculations to the free air calculations indicate that previous tree breakage calculations shown in Fig. 2.2 which were based on a linear decay are not considered to be seriously in error. The trend indicated by these calculations should be reasonably correct; however, magnitudes must be adjusted by experiment as was done in Figs. 4.3 and 4.4.

5.5 SCRATCH GAGE DATA

Scratch gage installations were made to provide basic data on maximum strain at base of tree stem and at base of crown to provide estimates of breakage-strain under impulsive loading, and to study the applicability of low-cost, strain-measuring instruments.

Preliminary analysis of scratch gage data indicates that: (1) Large deflections resulted in considerable distortion of the strain curve across the 1-ft section as would be expected from curved beam theory, and (2) greater strain occurred at the base of crown which adds to the evidence that breakage will occur near this point.

Figure 4.11 establishes one-to-one correspondence between strain meter and scratch gage readings. These data were taken at low deflection from a record similar to Fig. 4.10 and are maximum tension to maximum compression readings. The maximum strain level represented is therefore 3 μ in./in., and the readings are not influenced by nonlinearity of strain across the section of the tree stem, which occurs at high deflections.

Accuracy of scratch gage readings is dependent primarily on the establishment of zero reading, i.e., zero strain level prior to shock arrival. As shown in Fig. 4.10 this line is rather wide. Although readings were made to the nearest 0.1 μ in./in. of strain, estimated accuracy on the basis of Fig. 4.11 and difficulty in establishing zero is of the order of 0.5 μ in./in.

5.6 INSTRUMENTATION

5.6.1 Snubbers

Snubbers are the easiest and least costly way to measure maximum deflection. Field data can be read quickly and accurately. Reduction of these data to maximum deflection, however, requires that the arc traveled by the reference point be known. This difficulty has been overcome in recent static breakage tests by attaching two snubbers at the reference point, and thus determining maximum deflection directly from field measurements. Snubbers can be used to instrument an entire stand of trees, natural or artificial, which will be exposed to atomic explosions.

5.6.2 Scratch Gages

Scratch gages represent an expedient method of recording maximum strain whenever time sequence is not important. Accuracy is approximately 1/10 that of strain meters but in view of low cost and small installation time ($4.00 and 1/2 hr per installation), this can be tolerated when a large amount of data is desired. Reduction of data requires a microscope and is rather tedious. Readable scratches are not always obtained (only 6 out of 70 used by Project 3.3 failed to record), but experience in setting scratch gage arm pressure reduces record loss to a minimum.

5.6.3 Oscillograph-Strain System

Oscillograph recording of strain meter and strain gage circuits provides accurate measurement of time variations in strain and deflection. This system was well-adapted to field use and suffered no damage from induced signals, shock, or sand. Amplifier gain settings were stable. Attachment of strain meters to trees was satisfactory as evidenced by the fact that records returned to their original pre-shock zero readings. Strain-time records may be obtained from any point in the tree stem by use of this system suitably protected against blast damage.

The principal deterrent to large-scale instrumentation to obtain strain-time history on many trees is cost. A complete oscillograph-strain system to record strain-time at one point may be duplicated at a cost of approximately $900 and requires one day to install after the shelter and conduits are in place.

5.6.4 Motion Pictures

Motion pictures provided general visual data on tree and lollipop movement following shock arrival but were only partially

satisfactory for measurement of deflection. Disparity between nominal film speed and actual film speed made determination of time sequence difficult. Had film speed been constant and known, the disparity concerning the dynamic pressure on Shot 4 could have been resolved from measurements of the displacement of vapor originating from the tree foliage. Dust obscured all motion at Station I and motion after the first maximum at other stations on Shot 3. Collapse of a temporary shelter cover at Station III on Shot 3 covered the camera lens before maximum deflections occurred. All prints of Shot 3 were fuzzy, which made it difficult to follow precisely the position of tree stems.

5.6.5 Lollipops

Lollipops represent instruments which respond to peak dynamic pressure and may prove valuable in determining this quantity within forest stands. Lollipops at Operation SNAPPER failed to respond as intended because of their twisting motion during large deflections. This difficulty can be resolved by selection of a beam cross-section of higher torsional radius of gyration or by a redesign on the principle of the ballistic pendulum. Consideration should be given to the possibility of making the lollipop portable to permit changes in its location between shots of a graded series.

CHAPTER 6

CONCLUSIONS AND RECOMMENDATIONS

6.1 CONCLUSIONS

1. Blast damage to forests from atomic explosions is primarily a function of aerodynamic drag of the particle velocity. This basic assumption was verified by results of Project 3.3.

2. A method of predicting tree breakage has been established and in part substantiated. This method relates tree breakage with two ratios: shock peak dynamic pressure to dynamic pressure for breakage due to steady wind; and the ratio of tree period to positive phase duration time.

3. Peak dynamic pressure is a more compatible parameter than peak overpressure for predicting atomic explosion blast damage to trees and structures which have comparatively long periods and are susceptible to damage by aerodynamic drag. Peak dynamic pressure criteria appear to be compatible with breakage and deflection results obtained in Mach and regular reflection regions, whereas peak overpressure alone does not permit correlation of results.

4. Coniferous tree crowns break up as a unit with stem breakage usually occurring near the base of the crown. Strain on the tree stem is greater at the base of crown than at the 1-ft level.

5. Peculiarities in breakage and deflection data on Shot 4 indicate that peak dynamic pressures experienced were greater than those calculated from measured peak overpressures.

6. Agreement between measured and calculated lollipop deflections for Shot 3 substantiate calculation methods used to predict tree motion and the use of free air particle velocity and density time history as approximations for Mach and regular reflection regions.

7. Applicability of a single-mass system to analytically predict tree motion following shock was confirmed by Project 3.3 results.

8. The lower limit of shock peak dynamic pressure for complete breakage of isolated conifers is estimated to be in the order of 0.7 psi when associated with 1-sec positive phase duration. This value of dynamic pressure corresponds to a sea level overpressure of 5.5 psi for

Mach reflection. Some breakage will occur at lower dynamic pressures because of statistical variations of static strength found in apparently sound tree stems and also because of stem defect such as rot or fire scar.

9. Lollipops represent an instrument capable of measuring the total impulse due to dynamic pressure of shock particle velocity.

10. Natural forests or prepared forest stands can be instrumented economically to study blast damage from atomic explosions with no requirement for outside power or timing signals. The strain meter system accurately records time history of strain, snubbers provide adequate measurement of maximum deflection, and scratch gages measure maximum strain.

6.2 RECOMMENDATIONS

6.2.1 Future Atom Bomb Field Tests

1. The period ratio (tree period to duration time) covered in Project 3.3 should be extended by using trees with longer periods and by increasing the range of duration time through a graded series of shots.

2. Incident and reflected overpressures for the regular reflection reg should continue to be reported in the 2- to 8-psi overpressure region. Values should be measured approximately 20 ft above the ground.

3. Dynamic pressure should be measured in preference to overpressure whenever such data are used for correlation against structural damage due primarily to aerodynamic drag.

4. Investigation of shock wave disturbance due to low burst height should be continued, particularly in relation to peak particle velocity and density.

5. Instrumentation:

(a) Portable lollipops should be designed for use in and around forest stands.

(b) Scratch gages should be used to investigate maximum strain along tree stems

6. Before a prepared stand is exposed to atomic explosions the problem of what minimum area will constitute a semi-infinite stand must be solved.

RESTRICTED DATA
ATOMIC ENERGY ACT 1946

6.2.2 Other Work

1. More static breakage tests are needed to establish variation in static strength of growing tree stems.

2. Laboratory tests should be made to determine deflection-strain relations to the point of failure for tree stems.

RESTRICTED DATA
ATOMIC ENERGY ACT 1946

APPENDIX A

CALCULATION METHODS

A.1 EQUATION OF MOTION — LOLLIPOPS

Lollipop motion under blast loading is assumed to be that of a simple spring mass system acting under external force due to aerodynamic drag of the after-shock particle velocity. Internal damping force is assumed negligible in comparison to other forces. The system is shown schematically in Fig. A.1.

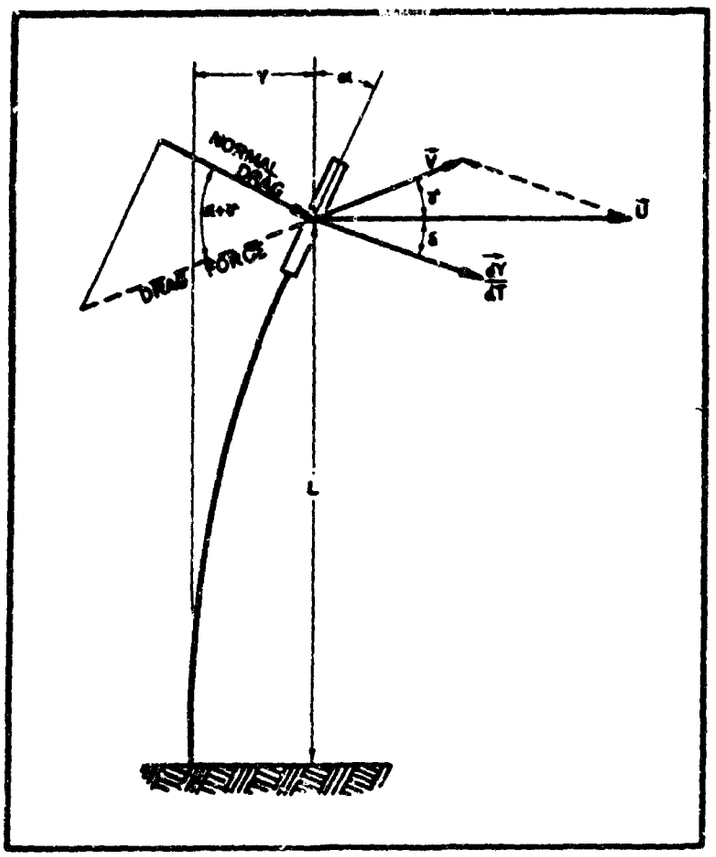

Fig. A.1 Equivalent Mechanical System — Lollipop

RESTRICTED DATA
ATOMIC ENERGY ACT 1943

From Newton's principle the equation of motion is

$$m\ddot{y} + k_\delta (y) = \left(\frac{\rho V^2}{2} C_D A\right)_\delta \tag{A.1}$$

where particle velocity relative to center of pressure velocity is given by

$$V^2 = U^2 + \dot{y}^2 - 2U\, y \cos\delta \tag{A.2}$$

and $\left(\frac{\rho V^2}{2} C_D A\right)_\delta$ is the drag component in the direction of motion. For small deflections the center of pressure follows a circular path and to the first approximation the beam assumes a sine curve. The angles are then

$$\delta \approx \frac{X}{L} \quad \text{and} \quad \alpha \approx \frac{\pi}{2}\frac{y}{L} \tag{A.3}$$

Referring to Fig. A.1 and combining Equations A.1 and A.2

$$m\ddot{y} + \frac{k}{\cos\delta} y = \frac{\rho_1 U_1^2}{2} C_D A \left(\frac{\rho}{\rho_1}\right) \left\{\left(\frac{U}{U_1}\right)^2 + \left(\frac{\dot{y}}{U_1}\right)^2 - \frac{2\dot{y}U}{U_1^2} \cos\delta\right\} \cos(\alpha+\gamma) \cos(\alpha-\gamma) \tag{A.4}$$

Letting

$$z = \frac{y}{Y_s}, \quad x = \frac{t}{T_+}, \quad \text{and} \quad \left(\frac{T}{2\pi}\right)^2 = \frac{m}{k}$$

where

$$Y_s = \frac{\rho_1 U_1^2 C_D A}{2k}$$

Equation A.4 can be written in dimensionless form:

$$\left(\frac{\mathcal{T}}{2\pi T_+}\right)^2 \ddot{z} + \frac{z}{\cos\delta} = \left(\frac{\rho}{\rho_1}\right)\left\{\left(\frac{U}{U_1}\right)^2 + \left(\frac{Y_s}{U_1T_+}\dot{z}\right)^2 - 2\left(\frac{Y_s}{U_1T_+}\dot{z}\right)\left(\frac{U}{U_1}\right)\cos\delta\right\}$$

$$\cos(\alpha+\gamma)\cos(\alpha-\gamma)$$

$$\gamma = \tan^{-1}\frac{\frac{Y_s}{U_1T_+}\dot{z}\sin\delta}{\frac{U}{U_1} - \frac{Y_s}{U_1T_+}\dot{z}\cos\delta} \qquad \text{(A.5)}$$

$$\delta = \frac{Y_s}{L} z$$

$$\alpha = \frac{\pi}{2}\frac{Y_s}{L} z$$

For free air $\frac{U}{U_1} = f_1(x)$ and $\frac{\rho-\rho_o}{\rho_1-\rho_o} = f_2(x)$ as shown in Fig. A.2. The density ratio may be found from the equation

$$\frac{\rho}{\rho_1} = 1 - \frac{\rho_1-\rho_o}{\rho_1}\left\{1 - f_2(x)\right\} \qquad \text{(A.6)}$$

Equations A.5 were integrated numerically for various values of $\frac{\mathcal{T}}{2\pi T_+}$, $\frac{Y_s}{U_1T_+}$, $\frac{Y_s}{L}$, and $\frac{P_1}{P_o}$ to establish maximum values z, $\frac{Y_m}{Y_s}$, and the time to reach this value, $\frac{T_m}{T_+}$, for a linear particle velocity and density

$$\frac{U}{U_1} = \frac{\rho-\rho_o}{\rho_1-\rho_o} = 1 - x$$

and for free air particle velocity and density relationships. The results of these calculations are shown in Fig. 4.9.

RESTRICTED DATA
ATOMIC ENERGY ACT 1946

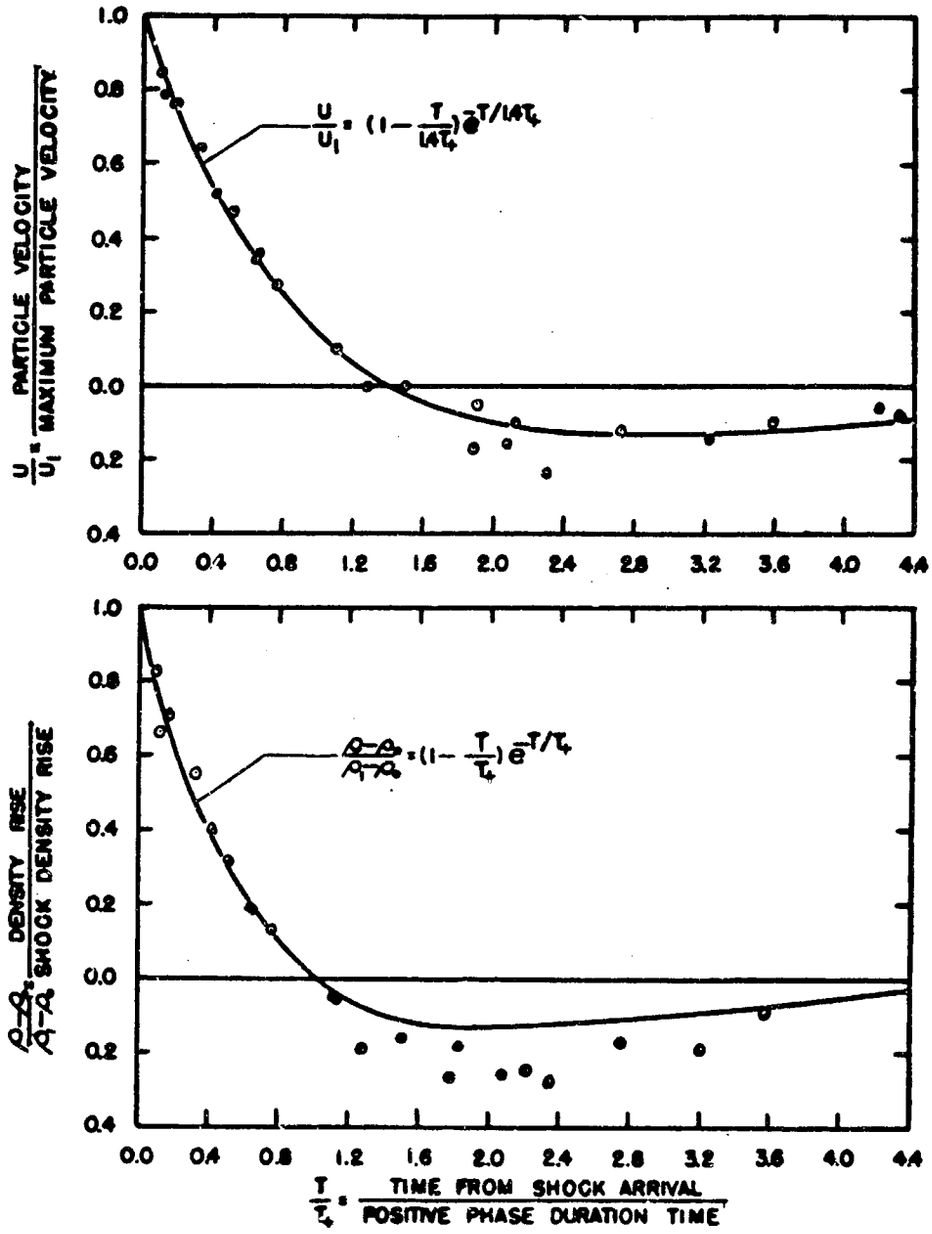

Fig. A.2 Theoretical Particle Velocity and Density Variation With Time for Free Air, $2.2 < (P_1 - P_o) < 8.4$ PSI. Equations Represent Empirical Fit Through Points Computed From L.A.S.L. IBM Problem M Calculations Supplied by Lt. Col. F. B. Porzel, Los Alamos Scientific Laboratory. Subscript o Refers to Preshock Values, Subscript 1 to Peak Values.

A.2 PEAK PARTICLE VELOCITY AND DENSITY FROM SHOCK EQUATIONS

A.2.1 Regular Reflection

For incident-reflected shock configurations (Fig. A.3) the density ratio may be found from

$$\frac{\rho_1}{\rho_0} = \frac{\mu^2 + \frac{P_2}{P_0}}{1 + \mu^2 \frac{P_2}{P_0}} \; \frac{\mu^2 + \frac{P_1}{P_2}}{1 + \mu^2 \frac{P_1}{P_2}} \tag{A.7}$$

since thermodynamic state equations are invariant under translation.[1/]

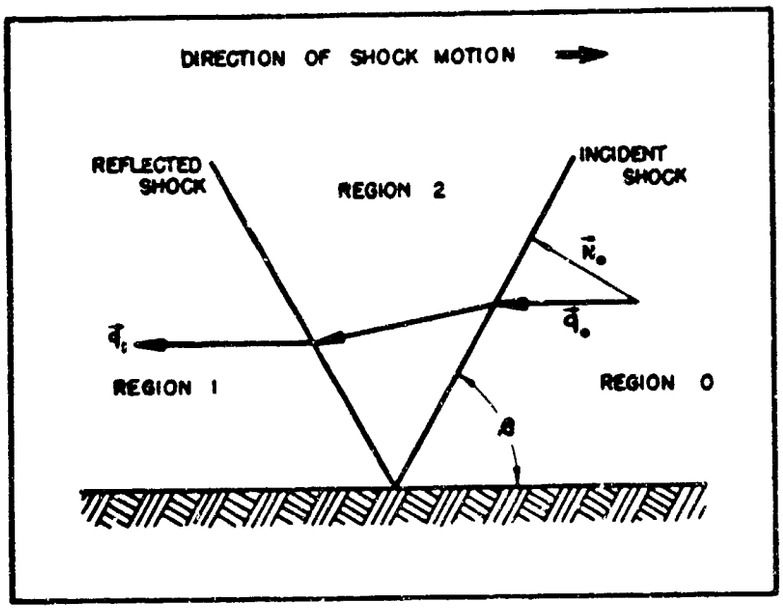

Fig. A.3 Incident-Reflected Shock in Stationary Frame of Reference

1/ R. Courant and K. O. Friedrichs. Supersonic Flow and Shock Waves. Interscience Publishers, Inc., New York, 1948. p. 302.

RESTRICTED DATA
ATOMIC ENERGY ACT 1946

Non-stationary oblique shock may be brought to rest by imposing a velocity q_o on the velocity field[2] (Fig. A.3) where

$$\left(\frac{q_o}{c_o}\right)^2 = \frac{1}{\sin^2\beta}\left(\frac{N_o}{c_o}\right)^2 = \frac{1}{\sin^2\beta}\,\frac{\mu^2 + \frac{P_2}{P_o}}{1+\mu^2} \qquad \text{(A.8)}$$

Angle of incidence, β, was determined from burst height and station ground distance.[3]

The peak particle velocity may then be found from the energy equation[4]

$$\mu^2\left(\frac{q_o}{c_o}\right)^2 + (1-\mu^2) = \mu^2\left(\frac{q_1}{c_o}\right)^2 + (1-\mu^2)\left(\frac{c_1}{c_o}\right)^2 \qquad \text{(A.9)}$$

where

$$\left(\frac{c_1}{c_o}\right)^2 = \frac{P_1}{P_o} \times \frac{\rho_o}{\rho_1}$$

and

$$\vec{q_1} = \vec{U_1} + \vec{q_o}$$

In order to make the calculation method entirely clear, a numerical example of dynamic pressure determination is presented. Consider the illustrative set of data:

burst height	= 2500 ft	P_o	= 13.0 psi
ground distance	= 3500 ft	ΔP_1	= 5.0 psi
c_o = 1100 ft/sec		ΔP_2	= 2.0 psi

2/ Ibid., pp. 148-149.
3/ This procedure was only approximate for Station II, Shot 3, where Mach reflection had formed, but the triple point was below the 10-ft level. For that pressure level $\beta - \beta_{extr} = 0.6^o$, which indicates that this approximation was reasonably correct.
4/ Courant and Friedrichs, op.cit., p. 302.

$$\beta = \tan^{-1}\frac{3500}{2500} = 54.5^{\circ}$$

$$\mu^2 = \frac{1}{6} \quad \text{for} \quad \gamma = 1.40$$

From Equation (A.7)

$$\frac{\rho_1}{\rho_o} = \frac{1 + 6\,\frac{15.0}{13.0}}{6 + \frac{15.0}{13.0}} \times \frac{1 + 6\,\frac{18.0}{15.0}}{6 + \frac{18.0}{15.0}} = 1.26$$

From Equation (A.8)

$$\left(\frac{q_o}{c_o}\right)^2 = \frac{1}{(.814)^2}\;\frac{1 + 6\,\frac{15.0}{13.0}}{7} = 1.709$$

From Equation (A.9)

$$\left(\frac{q_1}{c_o}\right)^2 = 1.709 + 5\left(1 - \frac{18.0}{13.0} \times \frac{1}{1.26}\right) = 1.219$$

Hence

$$U_1 = \left(\frac{q_1}{c_o} - \frac{q_o}{c_o}\right) c_o = (1.104 - 1.307)1100 = -224 \text{ ft/sec}$$

The dynamic pressure becomes

$$\frac{\rho_1 U_1^2}{2} = \frac{\rho_1}{\rho_o}\;\frac{\rho_o c_o^2}{2}\left(\frac{U_1}{c_o}\right)^2 = \frac{\gamma}{2}\;\frac{\rho_1}{\rho_o}\;P_o\left(\frac{U_1}{c_o}\right)^2$$

$$= 0.70 \times 1.26 \times 13.0\,(0.203)^2 = 0.473 \text{ psi}$$

RESTRICTED DATA
ATOMIC ENERGY ACT 1946

A.2.2 Mach Reflection

For a normal shock, Equations A.7 and A.9 can be written explicitly[5]

$$\frac{\rho_1}{\rho_o} = \frac{\mu^2 + \frac{P_1}{P_o}}{1 + \mu^2 \frac{P_1}{P_o}} \tag{A.10}$$

$$\left(\frac{U_1}{c_o}\right)^2 = \frac{(1 - \mu^2)^2 \left(\frac{P_1}{P_o} - 1\right)^2}{(1 + \mu^2)\left(\mu^2 + \frac{P_1}{P_o}\right)} \tag{A.11}$$

A.3 REDUCTION OF DEFLECTION DATA — LOLLIPOPS

To reduce experimental deflection data to dimensionless form, base fixity was computed from the spring constant based on the lollipop period, as given by Equation A.12, and the theoretical spring constant computed from the beam constants, assuming a fixed end cantilever and loading at the center of the disk.[6]

$$k_{\mathcal{T}} = \frac{4\pi^2}{g\mathcal{T}^2}\left(W_{disk} + \frac{33}{140} W_{beam}\right) \tag{A.12}$$

$$F = \frac{\text{spring constant from Eq. A.12}}{\text{computed spring constant for fixed end cantilever}} \tag{A.13}$$

$$\frac{1}{F} = \frac{\text{actual deflection}}{\text{theoretical deflection}} \tag{A.14}$$

The theoretical spring constant k under steady wind loading was computed using a distributed drag loading along the beam length equal to $\frac{\rho_1 U_1^2}{2} C_D A_f$ plus the drag due to the lollipop disk, $\frac{\rho_1 U_1^2}{2} C_D A_d$.

5/ Courant and Friedrichs, op.cit., pp. 148-149.
6/ S. Timoshenko. Vibration Problems in Engineering. (2nd ed.) D. Van Nostrand Company, Inc., New York, 1937. p. 86.

Drag coefficient was assumed to correspond to the steady state value[7] of 1.1 for the disk and 1.8 for the beam. The equivalent disk area then equals

$$A_{eq} = A_d \left(1 + \frac{\text{center of pressure deflection due to beam drag}}{\text{center of pressure deflection due to disk drag}}\right) \tag{A.15}$$

Actual static deflection corrected for base fixity becomes

$$Y_s = \frac{\rho_1 U_1^2}{2Fk} C_D A_{eq} \tag{A.16}$$

A.4 EQUATION OF MOTION — TREES

Trees are assumed to be simple spring mass systems with the same characteristics as previously described for lollipops except that the drag term is based on weight of dry crown and is a function of displacement.[8] An additional assumption is that the crown drag is independent of the angle of attack. Internal damping is neglected as experimentally determined values of the damping coefficient are negligible when compared with the crown drag force.

Calculations were carried out in a dimensional manner using Equation A.4 with the peak particle velocity, density, and positive phase duration time appropriate for each shot and station.

A.5 REDUCTION OF BREAKAGE DATA — TREES

Dimensionless breakage relationships presented in Figs. 4.3 and 4.4 may be inferred from the following analysis. From results of lollipop calculations the maximum deflection of a simple spring mass system may be represented to the first order as

$$\frac{Y_s}{Y_m} = f\left(\frac{\tau}{T_+}\right)$$

7/ Lionel S. Marks. Mechanical Engineers' Handbook. McGraw-Hill Book Company, New York, 1941. p. 1543.
8/ Forest Service, Analysis of Tree-Stem Breakage by Shock Wind—Ponderosa Pine, op. cit.

RESTRICTED DATA
ATOMIC ENERGY ACT 1946

Consider a completely linear system for which breakage occurs at a peak dynamic pressure of $\left(\frac{\rho_1 U_1^2}{2}\right)_b$. A static deflection may be defined on this basis:

$$(Y_s)_b = \left(\frac{\rho_1 U_1^2}{2}\right)_b \frac{C_D A}{k}$$

Under steady wind loading, breakage occurs at a dynamic pressure defined by

$$Y_b = \left(\frac{\rho U^2}{2}\right)_s \frac{C_D A}{k}$$

If under impulsive loading breakage occurs at the same deflection as under static loading by steady wind, then Y_m must equal Y_b. Therefore,

$$(Y_s)_b = Y_b \, f\left(\frac{\tau}{T_+}\right)$$

Hence

$$\frac{\left(\frac{\rho_1 U_1^2}{2}\right)_b}{\left(\frac{\rho U^2}{2}\right)_s} = f\left(\frac{\tau}{T_+}\right) \qquad \text{(A.17)}$$

For tree breakage the system is not linear to breakage. Nevertheless, the dimensionless relationship inferred in Equation A.17 may be applied intuitively provided it is realized that the functional relationship may not be the same.

NOMENCLATURE

A_d = lollipop disk area, sq ft

A_{eq} = equivalent lollipop disk area, sq ft

A_f = lollipop beam area per ft of length, sq ft/ft

c_o = sound speed at prevailing atmospheric conditions, ft/sec

c_1 = sound speed immediately behind shock wave, ft/sec

C_D = drag coefficient, dimensionless

$D(y)$ = drag function, sq ft

e = 2.718..., base of natural logarithms, dimensionless

f = a functional relation

F = base fixity, dimensionless

g = gravitational constant, ft/sec^2

k = spring constant for horizontal loading, lb/ft

k_f = spring constant determined from period of vibration, lb/ft

L = height of center of mass above ground, ft

m = mass, lb/sec^2/ft

N_o = flow velocity normal to incident shock, ft/sec

P_o = ambient air pressure, lb/sq in

P_1 = air pressure immediately behind shock, lb/sq in

P_2 = air pressure immediately behind incident shock, lb/sq in

q_o = flow velocity ahead of shock, Fig. A.3, ft/sec

q_1 = flow velocity behind shock, Fig. A.3, ft/sec

$R(y)$ = restoring force function, lb

t = time, sec

RESTRICTED DATA
ATOMIC ENERGY ACT 1946

T_m = time to maximum deflection, sec

T_+ = positive phase duration, sec

U = particle velocity, ft/sec

U_1 = maximum particle velocity behind shock, ft/sec

V = relative velocity, ft/sec

W = weight, lb

x = time parameter, t/T_+, dimensionless

y = mass displacement along arc, ft

$\dot{y}$ = dy/dt, ft/sec

$\ddot{y}$ = d^2y/dt^2, ft/sec^2

Y_b = deflection of center of mass at breakage, ft

Y_m = maximum deflection of center of mass, ft

Y_s = static deflection of center of mass associated with peak dynamic pressure, ft

z = deflection parameter, y/Y_s, dimensionless

$\dot{z}$ = dz/dx, dimensionless

$\ddot{z}$ = d^2z/dx^2, dimensionless

α = an angle, Fig. A.1, radians

β = angle of incident shock, radians

γ = an angle, Fig. A.1, radians

δ = an angle, Fig. A.1, radians

μ^2 = $\frac{\gamma - 1}{\gamma + 1}$, where γ is the ratio of specific heat of air, dimensionless

π = 3.1416..., dimensionless

ρ = air density, lb sec^2/ft^4

SUPPLEMENTARY

INFORMATION

Defense Nuclear Agency
6801 Telegraph Road
Alexandria, Virginia 22310-3398

IMTI 5 May 1994

MEMORANDUM FOR DEFENSE TECHNICAL INFORMTION CENTER
ATTN: OCD/MR. BILL BUSH

ERRATA

SUBJECT: Classification Review of WT-509

Reference DTIC accession no.#801308L.

The Defense Nuclear Agency Security Office has declassified the referenced report (WT-509).

The following distribution statement applies:

Approval for#public release.

FOR THE DIRECTOR:

ERRATA -AD- 801 308L

G. RUBINK
Chief, Technical Library

151.20/14